

Published in IET Control Theory and Applications
 Received on 23rd March 2008
 Revised on 11th November 2008
 doi: 10.1049/iet-cta.2008.0103



Approximation-based control of uncertain helicopter dynamics

S.S. Ge B. Ren K.P. Tee T.H. Lee*

Department of Electrical and Computer Engineering, National University of Singapore, Singapore 117576

*Institute for Infocomm Research, A*STAR, Singapore 138632

E-mail: samge@nus.edu.sg

Abstract: In this study, the altitude and yaw angle tracking is considered for a scale model helicopter, mounted on an experimental platform, in the presence of model uncertainties, which may be caused by unmodelled dynamics, or aerodynamical disturbances from the environment. To deal with the uncertainties, approximation-based techniques using neural network (NN) are proposed. In particular, two different types of NN, namely multilayer neural network and radial basis function neural network are adopted in control design and stability analysis. Based on Lyapunov synthesis, the proposed adaptive NN control ensures that both the altitude and the yaw angle track the given bounded reference signals to a small neighbourhood of zero, and guarantees semiglobal uniform ultimate boundedness of all the closed-loop signals at the same time. The effectiveness of the proposed control is illustrated through extensive simulations. Compared with the model-based control, approximation-based control yields better tracking performance in the presence of model uncertainties.

1 Introduction

Helicopters are inherently unstable without closed-loop control, different from many classes of mechanical systems that are naturally passive or dissipative. Unrestrained helicopter motion is governed by underactuated configuration i.e. the number of control inputs is less than the number of degrees of freedom to be stabilised, which makes it difficult to apply the conventional robotics approach for controlling Euler–Lagrange systems. In addition, the helicopter dynamics are highly nonlinear and strongly coupled, such that disturbances along a single degree of freedom can easily propagate to the other degrees of freedom and lead to loss of performance or even destabilisation. Therefore ensuring stability in helicopter flight is a challenging problem for nonlinear control design and development.

Increasing effort has been made towards control design that guarantees stability for helicopter systems. Many techniques have been proposed in the literature for the motion control of helicopters, which range from feedback linearisation to model reference adaptive control and dynamic inversion. Dynamic sliding mode control was proposed for helicopter vertical regulation in [1]. Output

tracking with nonhyperbolic and near nonhyperbolic internal dynamics in helicopter hover control was discussed in [2]. In [3], approximate input–output linearisation was employed to obtain a dynamically linearisable helicopter system without zero-dynamics, and output tracking was achieved. In [4], a high-bandwidth H_∞ loop shaping control was designed and tested for a robotic helicopter. Internal model-based control was applied to the nonlinear motion control of a helicopter in [5]. In [6], model-based control was applied to the altitude and yaw angle tracking of a Lagrangian helicopter model. Since helicopter control applications are characterised by unknown aerodynamical disturbances, it is generally difficult to model accurately. The presence of modelling errors, in the form of parametric and functional uncertainties, unmodelled dynamics and disturbances from the environment, is a common problem. In this context, model-based control, such as the aforementioned schemes, tends to be susceptible to uncertainties and disturbances that cause performance degradation. How to handle model uncertainties and disturbances is one of the important issues in the control of helicopters. Owing to the universal approximation capabilities, learning and adaptation, parallel distributed structures of neural networks (NNs), the feasibility of

applying NN to model unknown functions in dynamic systems has been demonstrated in several studies [7–12]. As such, several flight control approaches using NN have been proposed. Among of them, approximate dynamic inversion with augmented NN was proposed to handle unmodelled dynamics in [13–15], whereas neural dynamic programming was shown to be effective for tracking and trimming control of helicopters in [16]. During the adaptive trajectory control of autonomous helicopter in [17] and [18], the method of pseudocontrol hedging was used to protect the adaptation process from actuator limits and dynamics. In [19], MIMO output feedback adaptive NN control was proposed for an autonomous scale model helicopter mounted in a 2-degree-of-freedom (2DOF) platform. In [20], robust adaptive NN based on the mean value theorem and the implicit function theorem was proposed to handle the nonaffine nonlinearities in the helicopter dynamics without the construction of the dynamic inversion.

In this paper, motivated by [6], where the exact model dynamics are known, we consider the altitude and yaw angle tracking for a scale model helicopter mounted on an experimental platform in the presence of model uncertainties, which may be caused by unmodelled dynamics, sensor errors or aerodynamical disturbances from the environment. Compared with the model-based control used in [6], approximation-based control using NN, proposed in this paper, can accommodate the presence of model uncertainties, reduce the dependence on accurate model building, and thus, lead to the tracking performance improvement.

2 Problem formulation and preliminaries

In the following study, $(\tilde{\cdot}) = (\hat{\cdot}) - (\cdot)$, let $\|\cdot\|$ denote the 2-norm, $\|\cdot\|_F$ denote the Frobenius norm and $|\cdot|_1$ denote 1-norm, i.e. given $A = [a_{ij}] \in R^{m \times n}$, $\|A\|_F^2 = \text{tr}\{A^T A\} = \sum_{i,j} a_{i,j}^2$, and $|A|_1 = \sum_{i,j} |a_{i,j}|$. The following definition and technical lemma are required in the subsequent control design and stability analysis.

Definition 1 [11]: The solution $X(t)$ is semiglobally uniformly ultimately bounded (SGUUB) if, for any compact set Ω_0 and all $X(t_0) \in \Omega_0$, there exists an $\mu > 0$ and $T(\mu, X(t_0))$ such that $\|X(t)\| \leq \mu$ for all $t \geq t_0 + T$.

Lemma 1: For $a, b \in R^+$, the following inequality holds

$$\frac{ab}{a+b} \leq a \tag{1}$$

2.1 Helicopter dynamics

In this paper, we consider a VARIO scale model helicopter [6] which is mounted on an experimental platform as shown in Fig. 1, where the xyz and $x_1y_1z_1$ reference systems represent

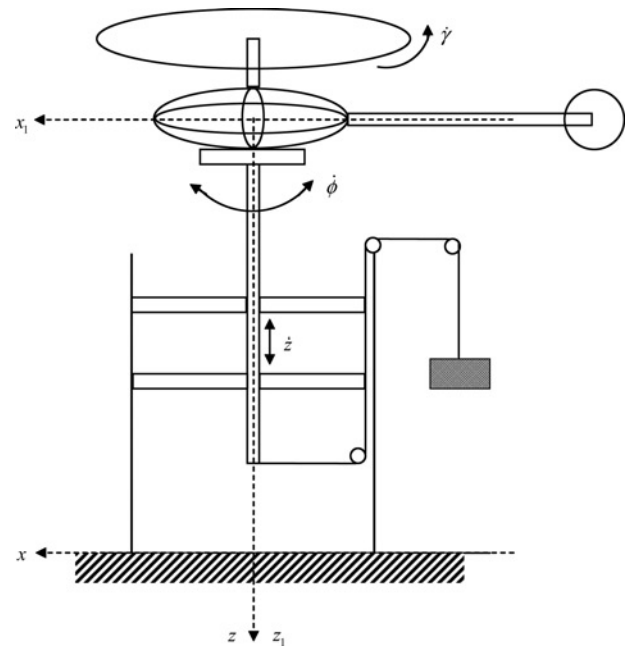


Figure 1 Helicopter-platform [6]

an inertial frame and a body fixed one, respectively. In addition, $\dot{\phi}$ is the yaw rate and $\dot{\gamma}$ is the main rotor angular velocity. The counterbalance weight compensates for the weight of the vertical column of the platform. The helicopter dynamics is described by Lagrangian formulation in the following [6]

$$D(q)\ddot{q} + C(q, \dot{q})\dot{q} + F(\dot{q}) + G(q) + \Delta(q, \dot{q}) = B(\dot{q})\tau \tag{2}$$

where q, \dot{q} and \ddot{q} are referred as the vectors of generalised coordinates, generalised velocities and generalised accelerations, respectively. In particular, $q = [q_1, q_2, q_3]^T = [z, \phi, \gamma]^T$ with z as the attitude ($z > 0$ downwards), ϕ as the yaw angle and γ as the main rotor azimuth angle; $\dot{q} = [\dot{q}_1, \dot{q}_2, \dot{q}_3]^T = [\dot{z}, \dot{\phi}, \dot{\gamma}]^T$ with \dot{z} as the vertical velocity, $\dot{\phi}$ as the yaw rate and $\dot{\gamma}$ as the main rotor angular velocity; $\ddot{q} = [\ddot{q}_1, \ddot{q}_2, \ddot{q}_3]^T = [\ddot{z}, \ddot{\phi}, \ddot{\gamma}]^T$ with \ddot{z} as the vertical acceleration $\ddot{\phi}$ as the yaw acceleration and $\ddot{\gamma}$ as the main rotor angular acceleration; $D(q) \in R^{3 \times 3}$ is the inertia matrix; $C(q, \dot{q})\dot{q} \in R^{3 \times 1}$ is the vector of Coriolis and centrifugal forces; $F(\dot{q}) \in R^{3 \times 1}$ is the vector of friction forces; $G(q) \in R^{3 \times 1}$ is the vector of gravitational forces; $\Delta(q, \dot{q}) \in R^{3 \times 1}$ is the vector of the model uncertainties, which may be caused by unmodelled dynamics, sensor errors or aerodynamical disturbances from the environment; $B(\dot{q}) \in R^{3 \times 2}$ is the matrix of control coefficients; and the control inputs $\tau = [\tau_1, \tau_2]^T \in R^{2 \times 1}$ are the main and tail rotor collectives (swash plate displacements), respectively. By exploiting the physical properties of the helicopter, e.g. how the control inputs are distributed to the helicopter dynamics, or the coupling relationship between the states, better performance can be achieved. To this end, we assume partial knowledge of the structure of the dynamics [6], although

the functions and parameters involved are unknown. The matrix coefficients are given by

$$\begin{aligned}
 D(q) &= \begin{bmatrix} d_{11} & 0 & 0 \\ 0 & d_{22}(q_3) & d_{23} \\ 0 & d_{23} & d_{33} \end{bmatrix} \\
 C(q, \dot{q}) &= \begin{bmatrix} 0 & 0 & 0 \\ 0 & c_{22}(q_3, \dot{q}_3) & c_{23}(q_3, \dot{q}_2) \\ 0 & c_{32}(q_3, \dot{q}_2) & 0 \end{bmatrix} \\
 F(\dot{q}) &= \begin{bmatrix} f_1(\dot{q}_3) \\ 0 \\ f_3(\dot{q}_3) \end{bmatrix}, \quad G(q) = \begin{bmatrix} g_1 \\ 0 \\ g_3 \end{bmatrix} \\
 \Delta(q, \dot{q}) &= \begin{bmatrix} \Delta_1(q, \dot{q}) \\ \Delta_2(q, \dot{q}) \\ \Delta_3(q, \dot{q}) \end{bmatrix}, \quad B(\dot{q}) = \begin{bmatrix} b_{11}(\dot{q}_3) & 0 \\ 0 & b_{22}(\dot{q}_3) \\ b_{31}(\dot{q}_3) & 0 \end{bmatrix}
 \end{aligned} \tag{3}$$

where d_{11} , d_{23} , d_{33} , g_1 , g_3 are unknown constants, $d_{22}(q_3)$, $c_{22}(q_3, \dot{q}_3)$, $c_{23}(q_3, \dot{q}_2)$, $c_{32}(q_3, \dot{q}_2)$, $f_1(\dot{q}_3)$, $f_3(\dot{q}_3)$, $b_{11}(\dot{q}_3)$, $b_{22}(\dot{q}_3)$, $b_{31}(\dot{q}_3)$, $\Delta_1(q, \dot{q})$, $\Delta_2(q, \dot{q})$ and $\Delta_3(q, \dot{q})$ are unknown functions. To facilitate control design in Section 3, the following assumptions are in order:

Assumption 1: The terms d_{11} and $d_{22}(q_3)d_{33} - d_{23}^2/2d_{33}$ are positive.

Assumption 2: The following equation $\dot{d}_{22}(q_3) - 2c_{22}(q_3, \dot{q}_3) = 0$ holds.

Remark 1: It is easily known that the helicopter model in (2) with the parameters given in [6], which will be used in the subsequent simulation section, satisfies both Assumptions 1 and 2.

Assumption 3: The signs of $b_{11}(\dot{q}_3)$ and $b_{22}(\dot{q}_3)$ are known. Without losing generality, assume that $b_{11}(\dot{q}_3)$ is positive and $b_{22}(\dot{q}_3)$ is negative. There exist positive constants \underline{b}_{11} and \underline{b}_{22} , such that $0 < \underline{b}_{11} \leq |b_{11}(\dot{q}_3)|$ and $0 < \underline{b}_{22} \leq |b_{22}(\dot{q}_3)|$.

Remark 2: In this paper, the vertical flight mode after take-off is considered. From physical analysis, to lift the helicopter up for flight operation, $|\dot{q}_3|$ has to be larger than some certain positive value (e.g. c_0) to overcome the gravity. It is noted that in the specific helicopter model given in (2) with the parameters given in [6], $b_{11}(\dot{q}_3) = 3.411\dot{q}_3^2 \geq 3.411c_0^2 > 0$. Therefore, there always exists some positive constant \underline{b}_{11} such that $0 < \underline{b}_{11} \leq |b_{11}(\dot{q}_3)|$ during the vertical flight mode. Similar analysis can be applied to $b_{22}(\dot{q}_3)$ as in Assumption 3.

Assumption 4: There exist positive constants \underline{d}_{22} and \bar{d}_{22} , such that $\underline{d}_{22} \leq |d_{22}(q_3)| \leq \bar{d}_{22}$.

Remark 3: Assumption 4 is reasonable due to $d_{22}(q_3) = 0.4305 + 0.0003 \cos^2(-4.143q_3)$ in the specific helicopter

model given in (2), which will be used in the subsequent simulation section.

The control objective is to ensure the tracking errors for the altitude $q_1(t)$ and yaw angle $q_2(t)$ from their respective desired trajectories $q_{1d}(t)$ and $q_{2d}(t)$ are driven to a small neighbourhood of zero, i.e. $|q_i(t) - q_{id}(t)| \leq \varepsilon_i$, where $\varepsilon_i > 0$, $i = 1, 2$. At the same time, the main rotor angular velocity $\dot{q}_3(t)$ is to remain bounded.

Assumption 5: The desired trajectories $q_{1d}(t)$ and $q_{2d}(t)$ and their time derivatives up to the third order are continuously differentiable and bounded for all $t \geq 0$.

2.2 Function approximation using NN

Due to the existence of model uncertainties in (2), we introduce NN here to approximate and compensate for them using the good function approximation capability of NN. In particular, two types of NN will be discussed, i.e. the radial basis function neural network (RBFNN), which is linearly parameterised; and the multilayer neural network (MNN), which is nonlinearly parameterised.

2.2.1 Function approximation using RBFNN: The RBFNN can be used to approximate the continuous function $f(Z): R^m \rightarrow R$ as follows

$$f(Z) = W^T S(Z) + \varepsilon(Z) \tag{4}$$

where the input vector $Z \in \Omega_Z \subset R^m$; weight vector $W = [w_1, w_2, \dots, w_l]^T \in R^l$, the NNs node number $l > 1$; $S(Z) = [s_1(Z), \dots, s_l(Z)]^T$, with $s_i(Z)$ being chosen as the commonly used Gaussian functions, which have the form

$$s_i(Z) = \exp\left[\frac{-(Z - \mu_i)^T(Z - \mu_i)}{\eta_i^2}\right], \quad i = 1, 2, \dots, l \tag{5}$$

where $\mu_i = [\mu_{i1}, \mu_{i2}, \dots, \mu_{im}]^T$ is the centre of the receptive field and η_i is the width of the Gaussian function; and $\varepsilon(Z)$ is the approximation error which is bounded over the compact set Ω_Z , i.e. $|\varepsilon(Z)| \leq \bar{\varepsilon}$, $\forall Z \in \Omega_Z$ where $\bar{\varepsilon} > 0$ is an unknown constant.

It has been proven that RBFNN (4) can approximate any continuous function $f(Z)$ over a compact set $\Omega_Z \subset R_m$ to any degree of accuracy as

$$f(Z) = W^{*T} S(Z) + \varepsilon^*(Z), \quad \forall Z \in \Omega_Z \subset R^m \tag{6}$$

where W^* is ideal constant weights and $\varepsilon^*(Z)$ is the approximation error for the special case where $W = W^*$.

Assumption 6: On the compact set Ω_Z , the ideal NN weights W^* are bounded by

$$\|W^*\| \leq w_m \tag{7}$$

The ideal weight vector W^* is defined as the value of W that minimises $|\varepsilon(Z)|$ for all $Z \in \Omega_Z \subset R^m$, i.e.

$$W^* = \arg \min_W \left\{ \sup_{Z \in \Omega_Z} |f(Z) - W^T S(Z)| \right\}$$

In general, the ideal weights W^* are unknown and need to be estimated in control design. Let \hat{W} be the estimates of W^* , and the weight estimation errors $\tilde{W} = \hat{W} - W^*$.

2.2.2 Function approximation using MNN: In this paper, we also consider nonlinearly parameterised MNN, which is used to approximate the continuous function $f(Z): R^m \rightarrow R$ as follows

$$f(Z) = W^T S(V^T Z) + \varepsilon(Z)$$

where the vector $Z = [z_1, z_2, \dots, z_m, 1]^T \in \Omega_Z \subset R^{m+1}$ are the input variables to the NNs; $S(\cdot) \in R^l$ is a vector of known continuous basis functions, with l denoting the number of neural nodes; $W \in R^l$ and $V \in R^{(m+1) \times l}$ are adaptable weights; and $\varepsilon(Z)$ is the approximation error which is bounded over the compact set Ω_Z , i.e. $|\varepsilon(Z)| \leq \bar{\varepsilon}$, $\forall Z \in \Omega_Z$ where $\bar{\varepsilon} > 0$ is an unknown constant. According to the universal approximation property [21], MNN can smoothly approximate any continuous function $f(Z)$ over a compact set $\Omega_Z \subset R^{m+1}$ to arbitrary any degree of accuracy as that

$$f(Z) = W^{*T} S(V^{*T} Z) + \varepsilon^*(Z), \quad \forall Z \in \Omega_Z \subset R^{m+1}$$

where W^* and V^* are the ideal constant weights, and $\varepsilon^*(Z)$ is the approximation error for the special case where $W = W^*$ and $V = V^*$. The ideal weights W^* and V^* are defined as the values of W and V that minimise $|\varepsilon(Z)|$ for all $Z \in \Omega_Z \subset R^{m+1}$, i.e.

$$(W^*, V^*) := \arg \min_{(W, V)} \left\{ \sup_{Z \in \Omega_Z} |f(Z) - W^T S(V^T Z)| \right\}$$

Assumption 7: On the compact set Ω_Z , the ideal NN weights W^* , V^* are bounded by

$$\|W^*\| \leq w_m, \quad \|V^*\|_F \leq v_m$$

In general, the ideal weights W^* and V^* are unknown and need to be estimated in control design. Let \hat{W} and \hat{V} be the estimates of W^* and V^* , respectively, and the weight estimation errors $\tilde{W} = \hat{W} - W^*$ and $\tilde{V} = \hat{V} - V^*$.

Lemma 2 [11]: Using $f_{mnn} = \hat{W}^T S(\hat{V}^T Z)$ to approximate the ideal function $f(Z)$, its approximation error can be expressed as

$$\begin{aligned} & \hat{W}^T S(\hat{V}^T Z) - W^{*T} S(V^{*T} Z) \\ &= \tilde{W}^T (\hat{S} - \hat{S}' \hat{V}^T Z) + \hat{W}^T \hat{S}' \tilde{V}^T Z + d_u \end{aligned}$$

where $\hat{S} = S(\hat{V}^T Z)$, $\hat{S}' = \text{diag} \{ \hat{S}'_1, \hat{S}'_2, \dots, \hat{S}'_l \}$ with

$$\hat{S}'_i = S'(\hat{v}_i^T Z) = \frac{d[s(z_a)]}{dz_a} \Big|_{z_a = \hat{v}_i^T Z}$$

and the residual term d_u is bounded by

$$|d_u| \leq \|V^*\|_F \|Z\| \|\hat{W}^T \hat{S}'\|_F + \|W^*\| \|\hat{S}' \hat{V}^T Z\| + \|W^*\|_1$$

Throughout this paper, we employ sigmoidal functions as basis functions for the MNN, which are defined by

$$s_i(z_a) = \frac{1}{1 + e^{-\mu z_a}}, \quad i = 1, 2, \dots, l \quad (8)$$

where $\mu > 0$ is a design constant.

3 Control design

Motivated by the previous work on model-based control of helicopters [6], we will design adaptive neural control to accommodate the presence of uncertainties in the dynamics (2), appearing in the functions $D(q)$, $C(q, \dot{q})$, $F(\dot{q})$, $G(q)$, $\Delta(q, \dot{q})$ and $B(\dot{q})$. After some simple manipulations on (2) and (3), we can obtain three subsystems: q_1 subsystem (9), q_2 subsystem (10) and q_3 subsystem (11) as follows

$$d_{11} \ddot{q}_1 + f_1(\dot{q}_3) + g_1 + \Delta_1(q, \dot{q}) = b_{11}(\dot{q}_3) \tau_1 \quad (9)$$

$$\begin{aligned} & \frac{d_{22}(q_3)d_{33} - d_{23}^2}{d_{33}} \ddot{q}_2 + c_{22}(q_3, \dot{q}_3) \dot{q}_2 + c_{23}(q_3, \dot{q}_2) \dot{q}_3 \\ & + \Delta_2(q, \dot{q}) + \frac{d_{23}}{d_{33}} (b_{31}(\dot{q}_3) \tau_1 - c_{32}(q_3, \dot{q}_2) \dot{q}_2 \\ & - f_3(\dot{q}) - g_3 - \Delta_3(q, \dot{q})) = b_{22}(\dot{q}_3) \tau_2 \end{aligned} \quad (10)$$

$$\begin{aligned} & \frac{d_{22}(q_3)d_{33} - d_{23}^2}{d_{22}(q_3)} \ddot{q}_3 + c_{32}(q_3, \dot{q}_2) \dot{q}_2 + f_3(\dot{q}_3) + g_3 \\ & + \Delta_3(q, \dot{q}) + \frac{d_{23}}{d_{22}(q_3)} (b_{22}(\dot{q}_3) \tau_2 - c_{22}(q_3, \dot{q}_3) \dot{q}_2 \\ & - c_{23}(q_3, \dot{q}_2) \dot{q}_3 - \Delta_2(q, \dot{q})) = b_{31}(\dot{q}_3) \tau_1 \end{aligned} \quad (11)$$

In the following, we will analyse and design control for each subsystem. For clarity, define the tracking errors and the filtered tracking errors as

$$e_i = q_i - q_{id}, \quad r_i = \dot{e}_i + \lambda_i e_i \quad (12)$$

where λ_i is a positive number, $i = 1, 2$. Then, the boundedness of r_i guarantees the boundedness of e_i and \dot{e}_i [22–25]. To study the stability of e_i and \dot{e}_i , we only need to study the properties of r_i . In addition, the following computable signals are defined

$$\dot{q}_{ir} = \dot{q}_{id} - \lambda_i e_i, \quad \ddot{q}_{ir} = \ddot{q}_{id} - \lambda_i \dot{e}_i$$

3.1 RBFNN-based control

In this section, we will investigate the RBFNN-based control design by Lyapunov synthesis to achieve the control objective. Regarding the obtained three subsystems (9)–(11), our control design consists of three steps: first, we will design control τ_1 based on the q_1 subsystem (9) second, design τ_2 based on the q_2 subsystem (10) and τ_1 ; finally, analyse the stability of internal dynamics of q_3 subsystem (11).

3.1.1 q_1 subsystem: Since $\dot{q}_1 = \dot{q}_{1r} + r_1$, $\ddot{q}_1 = \ddot{q}_{1r} + \dot{r}_1$, (9) becomes

$$d_{11}\dot{r}_1 = b_{11}(\dot{q}_3)\tau_1 - f_{S1,1} \quad (13)$$

where

$$f_{S1,1} = d_{11}\ddot{q}_{1r} + f_1(\dot{q}_3) + g_1 + \Delta_1(q, \dot{q}) \quad (14)$$

is an unknown continuous function, which is approximated by RBFNN to arbitrary any accuracy as

$$f_{S1,1} = W_1^{*T} S_1(Z_1) + \varepsilon_1(Z_1) \quad (15)$$

where the input vector $Z_1 = [q_1, \dot{q}_1, q_2, \dot{q}_2, q_3, \dot{q}_3, \ddot{q}_{1d}, \ddot{q}_{1d}]^T \in \Omega_{Z1} \subset \mathbb{R}^8$; $\varepsilon_1(Z_1)$ is the approximation error satisfying $|\varepsilon_1(Z_1)| \leq \bar{\varepsilon}_1$, where $\bar{\varepsilon}_1$ is a positive constant; W_1^* are ideal constant weights satisfying $\|W_1^*\| \leq w_{1m}$, where w_{1m} is a positive constant; and $S_1(Z_1)$ are the basis functions. By using \hat{W}_1 to approximate W_1^* , the error between the actual and the ideal RBFNN can be expressed as

$$\hat{W}_1^T S_1(Z_1) - W_1^{*T} S_1(Z_1) = \tilde{W}_1^T S_1(Z_1) \quad (16)$$

where $\tilde{W}_1 = \hat{W}_1 - W_1^*$.

Consider the following Lyapunov function candidate

$$V_1 = \frac{1}{2}d_{11}r_1^2 + \frac{1}{2}\tilde{W}_1^T \Gamma_1^{-1} \tilde{W}_1 \quad (17)$$

The time derivative of (17) along (13) and (15) is given by

$$\begin{aligned} \dot{V}_1 &= d_{11}r_1\dot{r}_1 + \tilde{W}_1^T \Gamma_1^{-1} \dot{\tilde{W}}_1 \\ &= r_1[b_{11}(\dot{q}_3)\tau_1 - W_1^{*T} S_1(Z_1) - \varepsilon_1(Z_1)] + \tilde{W}_1^T \Gamma_1^{-1} \dot{\tilde{W}}_1 \end{aligned} \quad (18)$$

As W_1^* is a constant vector, we know that $\dot{\tilde{W}}_1 = \dot{\hat{W}}_1$. Therefore (18) becomes

$$\dot{V}_1 = r_1[b_{11}(\dot{q}_3)\tau_1 - W_1^{*T} S_1(Z_1) - \varepsilon_1(Z_1)] + \tilde{W}_1^T \Gamma_1^{-1} \dot{\hat{W}}_1 \quad (19)$$

Consider the following RBFNN based control law and RBFNN weight adaptation law

$$\tau_1 = -k_1 r_1 - \frac{r_1(\hat{W}_1^T S_1(Z_1))^2}{\hat{b}_{11}(|r_1 \hat{W}_1^T S_1(Z_1)| + \delta_1)} \quad (20)$$

$$\dot{\hat{W}}_1 = -\Gamma_1[S_1(Z_1)r_1 + \sigma_1 \hat{W}_1] \quad (21)$$

where $k_1 > 0$, $\delta_1 > 0$, $\Gamma_1 = \Gamma_1^T > 0$, and $\sigma_1 > 0$.

Remark 4: The above σ -modification adaptation law (21) can be replaced by ε -modification adaptation law like $\dot{\hat{W}}_1 = -\Gamma_1[S_1(Z_1)r_1 + \sigma_1|r_1 \hat{W}_1| \hat{W}_1]$ easily. The control design based on σ -modification adaptation law in this paper can be extended to the case based on ε -modification adaptation law without any difficulty.

Substituting (20) and (21) into (19), we have

$$\begin{aligned} \dot{V}_1 &= -k_1 b_{11}(\dot{q}_3) r_1^2 - \frac{b_{11}(\dot{q}_3) r_1^2 (\hat{W}_1^T S_1(Z_1))^2}{\hat{b}_{11} |r_1 \hat{W}_1^T S_1(Z_1)| + \delta_1} - r_1 W_1^{*T} \\ &\quad \times S_1(Z_1) - r_1 \varepsilon_1(Z_1) - r_1 \tilde{W}_1^T S_1(Z_1) - \sigma_1 \tilde{W}_1^T \hat{W}_1 \end{aligned} \quad (22)$$

According to Assumption 3 and (16), we can rewrite (22) as

$$\begin{aligned} \dot{V}_1 &\leq -k_1 \hat{b}_{11} r_1^2 - \frac{r_1^2 (\hat{W}_1^T S_1(Z_1))^2}{|r_1 \hat{W}_1^T S_1(Z_1)| + \delta_1} \\ &\quad - r_1 \hat{W}_1^T S_1(Z_1) - r_1 \varepsilon_1(Z_1) - \sigma_1 \tilde{W}_1^T \hat{W}_1 \\ &\leq -k_1 \hat{b}_{11} r_1^2 - \frac{r_1^2 (\hat{W}_1^T S_1(Z_1))^2}{|r_1 \hat{W}_1^T S_1(Z_1)| + \delta_1} \\ &\quad + |r_1 \hat{W}_1^T S_1(Z_1)| + |r_1| \varepsilon_1(Z_1) - \sigma_1 \tilde{W}_1^T \hat{W}_1 \end{aligned} \quad (23)$$

Noting that

$$-\frac{r_1^2 (\hat{W}_1^T S_1(Z_1))^2}{|r_1 \hat{W}_1^T S_1(Z_1)| + \delta_1} + |r_1 \hat{W}_1^T S_1(Z_1)| = \frac{|r_1 \hat{W}_1^T S_1(Z_1)| \delta_1}{|r_1 \hat{W}_1^T S_1(Z_1)| + \delta_1} \quad (24)$$

According to Lemma 1, we can obtain from (24) that

$$-\frac{r_1^2 (\hat{W}_1^T S_1(Z_1))^2}{|r_1 \hat{W}_1^T S_1(Z_1)| + \delta_1} + |r_1 \hat{W}_1^T S_1(Z_1)| \leq \delta_1 \quad (25)$$

By completion of squares and using Young's inequality, the following inequalities hold

$$-\sigma_1 \tilde{W}_1^T \hat{W}_1 \leq -\frac{\sigma_1}{2} \|\tilde{W}_1\|^2 + \frac{\sigma_1}{2} \|W_1^*\|^2 \quad (26)$$

$$|r_1| \varepsilon_1(Z_1) \leq \frac{r_1^2}{2c_1} + \frac{c_1 \varepsilon_1^2(Z_1)}{2} \leq \frac{r_1^2}{2c_1} + \frac{c_1 \bar{\varepsilon}_1^2}{2} \quad (27)$$

where c_1 is a positive constant. Substituting the above inequalities (25)–(27) into (23) leads to

$$\begin{aligned} \dot{V}_1 &\leq -\left(k_1 \underline{b}_{11} - \frac{1}{2c_1}\right)r_1^2 - \frac{\sigma_1}{2} \|\tilde{W}_1\|^2 + \delta_1 + \frac{c_1}{2} \bar{\varepsilon}_1^2 + \frac{\sigma_1}{2} w_{1m}^2 \\ &\leq -\frac{1}{2} d_{11} \frac{2k_1 \underline{b}_{11} - (1/c_1)}{d_{11}} r_1^2 - \frac{1}{2} \frac{\sigma_1}{\lambda_{\max}(\Gamma_1^{-1})} \\ &\quad \times \tilde{W}_1^T \Gamma_1^{-1} \tilde{W}_1 + \delta_1 + \frac{c_1}{2} \bar{\varepsilon}_1^2 + \frac{\sigma_1}{2} w_{1m}^2 \\ &\leq -\min\left\{\frac{2k_1 \underline{b}_{11} - (1/c_1)}{d_{11}}, \frac{\sigma_1}{\lambda_{\max}(\Gamma_1^{-1})}\right\} \\ &\quad \times \left[\frac{1}{2} d_{11} r_1^2 + \frac{1}{2} \tilde{W}_1^T \Gamma_1^{-1} \tilde{W}_1\right] + \delta_1 + \frac{c_1}{2} \bar{\varepsilon}_1^2 + \frac{\sigma_1}{2} w_{1m}^2 \\ &\leq -\lambda_{10} V_1 + \mu_{10} \end{aligned} \quad (28)$$

where $\lambda_{10} = \min\{(2k_1 \underline{b}_{11} - 1/c_1)/d_{11}, \sigma_1/\lambda_{\max}(\Gamma_1^{-1})\}$, $\mu_{10} = \delta_1 + \frac{c_1}{2} \bar{\varepsilon}_1^2 + \frac{\sigma_1}{2} w_{1m}^2$.

3.1.2 q_2 subsystem: Similar to Section 3.1.1, since $\dot{q}_2 = \dot{q}_{2r} + r_2$, $\ddot{q}_2 = \ddot{q}_{2r} + \dot{r}_2$, (10) becomes

$$\frac{d_{22}(q_3)d_{33} - d_{23}^2}{d_{33}} \dot{r}_2 + c_{22}(q_3, \dot{q}_3)r_2 = b_{22}(\dot{q}_3)\tau_2 - f_{s2,1} \quad (29)$$

where

$$\begin{aligned} f_{s2,1} &= \frac{d_{22}(q_3)d_{33} - d_{23}^2}{d_{33}} \ddot{q}_{2r} + c_{22}(q_3, \dot{q}_3)\dot{q}_{2r} + c_{23}(q_3, \dot{q}_2)\dot{q}_3 \\ &\quad + \Delta_2(q, \dot{q}) + \frac{d_{23}}{d_{33}}(b_{31}(\dot{q}_3)\tau_1 - c_{32}(q_3, \dot{q}_2)\dot{q}_2 \\ &\quad - f_3(\dot{q}_3) - g_3 - \Delta_3(q, \dot{q})) \end{aligned}$$

is an unknown function, which is approximated by RBFNN to arbitrary any accuracy as

$$f_{s2,1} = W_2^{*T} S_2(Z_2) + \varepsilon_2(Z_2) \quad (30)$$

where the input vector $Z_2 = [\tau_1, q_1, \dot{q}_1, q_2, \dot{q}_2, q_3, \dot{q}_3, q_{2d}, \dot{q}_{2d}, \ddot{q}_{2d}]^T \in \Omega_{Z_2} \subset R^{10}$, $\varepsilon_2(Z_2)$ is the approximation error satisfying $|\varepsilon_2(Z_2)| \leq \bar{\varepsilon}_2$, where $\bar{\varepsilon}_2$ is an unknown positive constant; W_2^* are unknown ideal constant weights satisfying $\|W_2^*\| \leq w_{2m}$, where w_{2m} is an unknown positive constant; and $S_2(Z_2)$ are the basis functions. By using \hat{W}_2 to approximate W_2^* , the error between the actual and the ideal RBFNN can be expressed as

$$\hat{W}_2^T S_2(Z_2) - W_2^{*T} S_2(Z_2) = \tilde{W}_2^T S_2(Z_2) \quad (31)$$

where $\tilde{W}_2 = \hat{W}_2 - W_2^*$.

To analyse the closed-loop stability for the q_2 subsystem, let

$$V_2 = \frac{1}{2} \frac{d_{22}(q_3)d_{33} - d_{23}^2}{d_{33}} r_2^2 + \frac{1}{2} \tilde{W}_2^T \Gamma_2^{-1} \tilde{W}_2 \quad (32)$$

Lemma 3: The function V_2 (32) is positive definite and decrescent, in the sense that there exist two time-invariant positive definite functions $\underline{V}_2(r_2, \tilde{W}_2)$ and $\bar{V}_2(r_2, \tilde{W}_2)$, such that

$$\underline{V}_2(r_2, \tilde{W}_2) \leq V_2 \leq \bar{V}_2(r_2, \tilde{W}_2)$$

Proof: Noting that the particular choice of V_2 in (32), a function of r_2 , \tilde{W}_2 and $d_{22}(q_3)$, is to establish the stability for r_2 and \tilde{W}_2 only; therefore, we regard $d_{22}(q_3)$ as a function of time. From Assumptions 1 and 4, we know that

$$0 < \frac{|d_{22}d_{33}| - d_{23}^2}{|d_{33}|} < \left| \frac{d_{22}(q_3)d_{33} - d_{23}^2}{d_{33}} \right| \leq \frac{\bar{d}_{22}|d_{33}| + d_{23}^2}{|d_{33}|} \quad (33)$$

Therefore there also exist time-invariant positive definite functions $\underline{V}_2(r_2, \tilde{W}_2)$ and $\bar{V}_2(r_2, \tilde{W}_2)$, such that $\underline{V}_2(r_2, \tilde{W}_2) \leq V_2 \leq \bar{V}_2(r_2, \tilde{W}_2)$, which implies that V_2 is also positive definite and decrescent, according to [25]. This completes the proof. \square

The time derivative of (32) is given as

$$\dot{V}_2 = \frac{1}{2} \dot{d}_{22}(q_3)r_2^2 + \frac{d_{22}(q_3)d_{33} - d_{23}^2}{d_{33}} r_2 \dot{r}_2 + \tilde{W}_2^T \Gamma_2^{-1} \dot{\tilde{W}}_2 \quad (34)$$

According to Assumption 2, (34) becomes

$$\dot{V}_2 = r_2 \left[\frac{d_{22}(q_3)d_{33} - d_{23}^2}{d_{33}} \dot{r}_2 + c_{22}(q_3, \dot{q}_3)r_2 \right] + \tilde{W}_2^T \Gamma_2^{-1} \dot{\tilde{W}}_2 \quad (35)$$

As W_2^* is a constant vector, it is easy to obtain that

$$\dot{\tilde{W}}_2 = \dot{\hat{W}}_2 \quad (36)$$

Substituting (29), (30) and (36) into (35), we have

$$\dot{V}_2 = r_2 [b_{22}(\dot{q}_3)\tau_2 - W_2^{*T} S_2(Z_2) - \varepsilon_2(Z_2)] + \tilde{W}_2^T \Gamma_2^{-1} \dot{\hat{W}}_2 \quad (37)$$

Consider the following RBFNN-based control law and RBFNN weight adaption law

$$\tau_2 = k_2 r_2 + \frac{r_2 (\hat{W}_2^T S_2(Z_2))^2}{\underline{b}_{22}(|r_2 \hat{W}_2^T S_2(Z_2)| + \delta_2)} \quad (38)$$

$$\dot{\hat{W}}_2 = -\Gamma_2 [S_2(Z_2)r_2 + \sigma_2 \hat{W}_2] \quad (39)$$

where $k_2 > 0, \delta_2 > 0, \Gamma_2 = \Gamma_2^T > 0$ and $\sigma_2 > 0$. Substituting (38) and (39) into (37), we have

$$\begin{aligned} \dot{V}_2 = & k_2 b_{22} (\dot{q}_3) r_1^2 + \frac{b_{22} (\dot{q}_3)}{b_{22}} \frac{r_2^2 (\hat{W}_2^T S_2(Z_2))^2}{|r_2 \hat{W}_2^T S_2(Z_2)| + \delta_2} - r_2 W_2^{*T} S_2(Z_2) \\ & - r_2 \varepsilon_2(Z_2) - r_2 \tilde{W}_2^T S_2(Z_2) - \sigma_2 \tilde{W}_2^T \hat{W}_2 \end{aligned} \quad (40)$$

According to Assumption 3 and (31), we can rewrite (40) as

$$\begin{aligned} \dot{V}_2 \leq & -k_2 b_{22} r_2^2 - \frac{r_2^2 (\hat{W}_2^T S_2(Z_2))^2}{|r_2 \hat{W}_2^T S_2(Z_2)| + \delta_2} \\ & - r_2 \hat{W}_2^T S_2(Z_2) - r_2 \varepsilon_2(Z_2) - \sigma_2 \tilde{W}_2^T \hat{W}_2 \\ \leq & -k_2 b_{22} r_2^2 - \frac{r_2^2 (\hat{W}_2^T S_2(Z_2))^2}{|r_2 \hat{W}_2^T S_2(Z_2)| + \delta_2} \\ & + |r_2 \hat{W}_2^T S_2(Z_2)| + |r_2 \varepsilon_2(Z_2)| - \sigma_2 \tilde{W}_2^T \hat{W}_2 \end{aligned} \quad (41)$$

Similar to (25), we have

$$-\frac{r_2^2 (\hat{W}_2^T S_2(Z_2))^2}{|r_2 \hat{W}_2^T S_2(Z_2)| + \delta_2} + |r_2 \hat{W}_2^T S_2(Z_2)| \leq \delta_2 \quad (42)$$

By completion of squares and using Young's inequality, the following inequalities hold

$$-\sigma_2 \tilde{W}_2^T \hat{W}_2 \leq -\frac{\sigma_2}{2} \|\tilde{W}_2\|^2 + \frac{\sigma_2}{2} \|W_2^*\|^2 \quad (43)$$

$$|r_2 \varepsilon_2(Z_2)| \leq \frac{r_2^2}{2c_2} + \frac{c_2 \varepsilon_2^2(Z_2)}{2} \leq \frac{r_2^2}{2c_2} + \frac{c_2 \bar{\varepsilon}_2^2}{2} \quad (44)$$

where c_2 is a positive constant. Substituting the above inequalities (42)–(44) into (41) leads to

$$\begin{aligned} \dot{V}_2 \leq & -\left(k_2 b_{22} - \frac{1}{2c_2}\right) r_2^2 - \frac{\sigma_2}{2} \|\tilde{W}_2\|^2 + \delta_2 + \frac{c_2 \bar{\varepsilon}_2^2}{2} + \frac{\sigma_2}{2} \omega_{2m}^2 \\ \leq & -\lambda_{20} V_2 + \mu_{20} \end{aligned} \quad (45)$$

where $\lambda_{20} = \min\{(2k_2 b_{22} - 1/c_2) |d_{33}| / (\bar{d}_{22} |d_{33}| + \bar{d}_{23}^2), \sigma_2 / \lambda_{\max}(\Gamma_2^{-1})\}$, $\mu_{20} = \delta_2 + \frac{c_2 \bar{\varepsilon}_2^2}{2} + \frac{\sigma_2}{2} \omega_{2m}^2$.

3.1.3 q_3 subsystem: Finally, using the designed control laws (20) and (38), the q_3 -subsystem (1) can be rewritten as

$$\dot{\eta} = \psi(\xi, \eta, u) \quad (46)$$

where $\eta = [q_3, \dot{q}_3]^T$, $\xi = [q_1, q_2, \dot{q}_1, \dot{q}_2]^T$, $u = [\tau_1, \tau_2]^T$.

Then, the zero-dynamics can be addressed as [26]

$$\dot{\eta} = \psi(0, \eta, u^*(0, \eta)) \quad (47)$$

where $u^* = [\tau_1^*, \tau_2^*]^T$.

Assumption 8 [26]: System (9) (10) (11) is hyperbolically minimum-phase, i.e. zero-dynamics (47) is exponentially stable. In addition, assume that the control input u is designed as a function of the states (ξ, η) and the reference signal satisfying Assumption 5, and the function $f(\xi, \eta, u)$ is Lipschitz in ξ , i.e. there exist constants L_ξ and L_f for $f(\xi, \eta, u)$ such that

$$\|f(\xi, \eta, u) - f(0, \eta, u_\eta)\| \leq L_\xi \|\xi\| + L_f \quad (48)$$

where $u_\eta = u^*(0, \eta)$.

Under Assumption 8, by the Converse Theorem of Lyapunov [27], there exists a Lyapunov function $V_0(\eta)$ which satisfies

$$\gamma_a \|\eta\|^2 \leq V_0(\eta) \leq \gamma_b \|\eta\|^2 \quad (49)$$

$$\frac{\partial V_0}{\partial \eta} f(0, \eta, u_\eta) \leq -\lambda_a \|\eta\|^2 \quad (50)$$

$$\left\| \frac{\partial V_0}{\partial \eta} \right\| \leq \lambda_b \|\eta\| \quad (51)$$

where $\gamma_a, \gamma_b, \lambda_a$ and λ_b are positive constants.

Lemma 4 [26]: For the internal dynamics $\dot{\eta} = f(\xi, \eta, u)$ of the system, if Assumption 8 is satisfied, and the states ξ are bounded by a positive constant $\|\xi\|_{\max}$, i.e. $\|\xi\| \leq \|\xi\|_{\max}$, then there exist positive constants L_η and T_0 , such that

$$\|\eta(t)\| \leq L_\eta, \quad \forall t > T_0 \quad (52)$$

Proof: According to Assumption 8, there exists a Lyapunov function $V_0(\eta)$. Differentiating $V_0(\eta)$ along (9), (10), and (11) yields

$$\begin{aligned} \dot{V}_0(\eta) &= \frac{\partial V_0}{\partial \eta} f(\xi, \eta, u) \\ &= \frac{\partial V_0}{\partial \eta} f(0, \eta, u_\eta) + \frac{\partial V_0}{\partial \eta} [f(\xi, \eta, u) - f(0, \eta, u_\eta)] \end{aligned} \quad (53)$$

Noting (48)–(51), (53) can be written as

$$\begin{aligned} \dot{V}_0(\eta) &\leq -\lambda_a \|\eta\|^2 + \lambda_b \|\eta\| (L_\xi \|\xi\| + L_f) \\ &\leq -\lambda_a \|\eta\|^2 + \lambda_b \|\eta\| (L_\xi \|\xi\|_{\max} + L_f) \end{aligned}$$

Therefore $\dot{V}_0(\eta) \leq 0$, whenever

$$\|\eta\| \geq \frac{\lambda_b}{\lambda_a} (L_\xi \|\xi\|_{\max} + L_f)$$

By letting $L_\eta = \lambda_b / r \lambda_a (L_\xi \|\xi\|_{\max} + L_f)$, we conclude that there exists a positive constant T_0 , such that (52) holds. \square

The following theorem shows the stability and control performance of the closed-loop system.

Theorem 1: Consider the closed-loop system consisting of the subsystems (9)–(11), the control laws (20), (38) and adaptation laws (21), (39). Under Assumptions 1–8, the overall closed-loop neural control system is SGUUB in the sense that all of the signals in the closed-loop system are bounded, and the tracking errors and neural weights converge to the following regions

$$\begin{aligned} |e_1| &\leq |e_1(0)| + \frac{1}{\lambda_1} \sqrt{\frac{2\mu_1}{d_{11}}}, \quad \|\hat{W}_1\| \leq \sqrt{\frac{2\mu_1}{\lambda_{\min}(\Gamma_1^{-1})}} + w_{1m} \\ |e_2| &\leq |e_2(0)| + \frac{1}{\lambda_2} \sqrt{\frac{2|d_{33}|\mu_2}{|d_{22}|d_{33}| - d_{23}^2}}, \\ \|\hat{W}_2\| &\leq \sqrt{\frac{2\mu_2}{\lambda_{\min}(\Gamma_2^{-1})}} + w_{2m} \end{aligned} \quad (54)$$

with

$$\mu_i = \frac{\mu_{i0}}{\lambda_{i0}} + V_i(0), \quad \mu_{i0} = \delta_i + \frac{1}{2} \bar{\varepsilon}_i^2 + \frac{\sigma_i}{2} w_{im}^2, \quad i = 1, 2$$

$$\lambda_{10} = \min\{(2k_1 \underline{b}_{11} - 1/c_1)/d_{11}, \sigma_1/\lambda_{\max}(\Gamma_1^{-1})\}$$

$$\lambda_{20} = \min\{(2k_2 - 1/c_2)|d_{33}|/(\bar{d}_{22}|d_{33}| + d_{23}^2), \sigma_2/\lambda_{\max}(\Gamma_2^{-1})\}$$

where $e_i(0)$ and $V_i(0)$ are initial values of $e_i(t)$ and $V_i(t)$, respectively.

Proof: Based on the previous analysis, the proof also proceeds by studying each subsystem in order. First, the closed-loop stability analysis of q_1 subsystem (9) with control τ_1 (20) and adaptation law (21) is made by using Lyapunov synthesis. Second, similar closed-loop stability will be achieved on q_2 subsystem (10) with τ_2 (38) and adaptation law (39). Finally, the stability analysis of internal dynamics of q_3 subsystem (11) is made based on the stability of the previous two subsystems.

q₁-subsystem: Solving the inequality (109), we have $0 \leq V_1(t) \leq \mu_1$ with $\mu_1 = (\mu_{10}/\lambda_{10}) + V_1(0)$. Then, from the definition of $V_1(t)$ (17), we can obtain

$$|r_1| \leq \sqrt{\frac{2\mu_1}{d_{11}}}, \quad \|\tilde{W}_1\| \leq \sqrt{\frac{2\mu_1}{\lambda_{\min}(\Gamma_1^{-1})}} \quad (55)$$

Since $\dot{e}_1 = -\lambda_1 e_1 + r_1$, solving this equation results in

$$e_1 = e^{-\lambda_1 t} e_1(0) + \int_0^t e^{-\lambda_1(t-\tau)} r_1 \, d\tau \quad (56)$$

According to (55) and (56), we have

$$|e_1| \leq |e_1(0)| + \frac{1}{\lambda_1} \sqrt{\frac{2\mu_1}{d_{11}}} \quad (57)$$

Noting $q_1 = e_1 + q_{1d}$, $\hat{W}_1 = \tilde{W}_1 + W_1^*$, $\|W_1^*\| \leq w_{1m}$ and Assumption 5, we obtain

$$|q_1| \leq |e_1| + |q_{1d}| \leq |e_1(0)| + \frac{1}{\lambda_1} \sqrt{\frac{2\mu_1}{d_{11}}} + |q_{1d}| \in L_\infty$$

$$\|\hat{W}_1\| \leq \|\tilde{W}_1\| + \|W_1^*\| \leq \sqrt{\frac{2\mu_1}{\lambda_{\min}(\Gamma_1^{-1})}} + w_{1m} \in L_\infty$$

Since the control τ_1 is a function of r_1 and \hat{W}_1 , its boundedness is also guaranteed.

q₂-subsystem: Similar to the analysis of q_1 subsystem, we have

$$|r_2| \leq \sqrt{\frac{2|d_{33}|\mu_2}{|d_{22}|d_{33}| - d_{23}^2}}, \quad \|\tilde{W}_2\| \leq \sqrt{\frac{2\mu_2}{\lambda_{\min}(\Gamma_2^{-1})}} \quad (58)$$

Furthermore, we obtain

$$|e_2| \leq |e_2(0)| + \frac{1}{\lambda_2} \sqrt{\frac{2|d_{33}|\mu_2}{|d_{22}|d_{33}| - d_{23}^2}}$$

$$|q_2| \leq |e_2| + |q_{2d}| \leq |e_2(0)|$$

$$+ \frac{1}{\lambda_2} \sqrt{\frac{2|d_{33}|\mu_2}{|d_{22}|d_{33}| - d_{23}^2}} + |q_{2d}| \in L_\infty$$

$$\|\hat{W}_2\| \leq \|\tilde{W}_2\| + \|W_2^*\| \leq \sqrt{\frac{2\mu_2}{\lambda_{\min}(\Gamma_2^{-1})}} + w_{2m} \in L_\infty \quad (59)$$

and thus the boundedness of control τ_2 .

q₃-subsystem: From the previous stability analysis about the q_1 subsystem and the q_2 subsystem, we know that q_1 , q_2 , \dot{q}_1 , \dot{q}_2 are bounded. Accordingly, ξ are bounded. According to Lemma 5, we know that the internal dynamics is stable, i.e. $\eta(q_3$ and $\dot{q}_3)$ are bounded. All the signals in the closed-loop system are bounded. This completes the proof. \square

3.2 MNN-based control

Nonlinearly parameterised approximators, such as MNN, can be linearised by Taylor series expansions, with the higher order terms being taken as part of the modelling error. Due to the nonlinear parameterisation, the control design and stability analysis involving MNN are more complex than that based on the linearly parameterised network RBFNN.

3.2.1 q_1 subsystem: Similar to the RBFNN case in Section 3.1.1, (9) is written as

$$d_{11}\dot{r}_1 = b_{11}(\dot{q}_3)\tau_1 - f_{S1,1} \quad (60)$$

where the unknown continuous function

$$f_{S1,1} = d_{11}\ddot{q}_{1r} + f_1(\dot{q}_3) + g_1 + \Delta_1(q, \dot{q}) \quad (61)$$

is approximated by MNN to arbitrary any accuracy as

$$f_{S1,1} = W_1^{*\text{T}} S_1(V_1^{*\text{T}} Z_1) + \varepsilon_1(Z_1) \quad (62)$$

where the input vector $Z_1 = [q_1, \dot{q}_1, q_2, \dot{q}_2, q_3, \dot{q}_3, \dot{q}_{1d}, \ddot{q}_{1d}, 1]^\text{T} \in \Omega_{Z_1} \subset R^9$; $\varepsilon_1(Z_1)$ is the approximation error satisfying $|\varepsilon_1(Z_1)| \leq \bar{\varepsilon}_1$, where $\bar{\varepsilon}_1$ is a positive constant; W_1^* and V_1^* are unknown ideal constant weights satisfying $\|W_1^*\| \leq w_{1m}$, $\|V_1^*\|_F \leq v_{1m}$, which are positive constants. By using $\hat{W}_1^\text{T} S_1(\hat{V}_1^\text{T} Z_1)$ to approximate $W_1^{*\text{T}} S_1(V_1^{*\text{T}} Z_1)$, the error between the actual and the ideal MNN can be expressed as

$$\begin{aligned} & \hat{W}_1^\text{T} S(\hat{V}_1^\text{T} Z_1) - W_1^{*\text{T}} S(V_1^{*\text{T}} Z_1) \\ &= \tilde{W}_1^\text{T} (\hat{S}_1 - \hat{S}'_1 \hat{V}_1^\text{T} Z_1) + \hat{W}_1^\text{T} \hat{S}'_1 \tilde{V}_1^\text{T} Z_1 + d_{u1} \end{aligned} \quad (63)$$

where $\hat{S}_1 = S(\hat{V}_1^\text{T} Z_1)$, $\hat{S}'_1 = \text{diag} \{ \hat{s}'_1, \hat{s}'_2, \dots, \hat{s}'_l \}$ with

$$\hat{s}'_i = s'(\hat{v}_i^\text{T} Z) = \frac{d[s(z_a)]}{dz_a} \Big|_{z_a = \hat{v}_i^\text{T} Z}$$

the residual term d_{u1} is bounded by

$$|d_{u1}| \leq \|W_1^*\|_F \|Z_1\| \hat{W}_1^\text{T} \hat{S}'_1 \|Z_1\| + \|W_1^*\| \|\hat{S}'_1 \hat{V}_1^\text{T} Z_1\| + |W_1^*|_1 \quad (64)$$

and the weight estimation errors $\tilde{W}_1 = \hat{W}_1 - W_1^*$, $\tilde{V}_1 = \hat{V}_1 - V_1^*$.

Consider the following Lyapunov function candidate

$$V_1(r_1, \tilde{W}_1, \tilde{V}_1) = \frac{1}{2} d_{11} r_1^2 + \frac{1}{2} \tilde{W}_1^\text{T} \Gamma_{W1}^{-1} \tilde{W}_1 + \frac{1}{2} \text{tr} \{ \tilde{V}_1^\text{T} \Gamma_{V1}^{-1} \tilde{V}_1 \} \quad (65)$$

The time derivative of (65) along (60) and (62) is given by

$$\begin{aligned} \dot{V}_1 &= r_1 [b_{11}(\dot{q}_3)\tau_1 - W_1^{*\text{T}} S_1(V_1^{*\text{T}} Z_1) - \varepsilon_1(Z_1)] \\ &+ \tilde{W}_1^\text{T} \Gamma_{W1}^{-1} \dot{\tilde{W}}_1 + \text{tr} \{ \tilde{V}_1^\text{T} \Gamma_{V1}^{-1} \dot{\tilde{V}}_1 \} \end{aligned} \quad (66)$$

As W_1^* , V_1^* are constant vectors, it is easy to obtain that

$$\dot{\tilde{W}}_1 = \dot{\hat{W}}_1, \quad \dot{\tilde{V}}_1 = \dot{\hat{V}}_1 \quad (67)$$

Substituting (67) into (66), we have

$$\begin{aligned} \dot{V}_1 &= r_1 [b_{11}(\dot{q}_3)\tau_1 - W_1^{*\text{T}} S_1(V_1^{*\text{T}} Z_1) - \varepsilon_1(Z_1)] \\ &+ \tilde{W}_1^\text{T} \Gamma_{W1}^{-1} \dot{\tilde{W}}_1 + \text{tr} \{ \tilde{V}_1^\text{T} \Gamma_{V1}^{-1} \dot{\tilde{V}}_1 \} \end{aligned} \quad (68)$$

Consider the following MNN-based control law and MNN weight adaption laws

$$\begin{aligned} \tau_1 &= -k_1 r_1 - \frac{r_1 (\hat{W}_1^\text{T} S(\hat{V}_1^\text{T} Z_1))^2}{\hat{b}_{11} (|r_1 \hat{W}_1^\text{T} S(\hat{V}_1^\text{T} Z_1)| + \delta_1)} \\ &- \frac{k_1 r_1}{\hat{b}_{11}} (\|Z_1 \hat{W}_1^\text{T} \hat{S}'_1\|_F^2 + \|\hat{S}'_1 \hat{V}_1^\text{T} Z_1\|^2) \end{aligned} \quad (69)$$

$$\dot{\hat{W}}_1 = -\Gamma_{W1} [(\hat{S}_1 - \hat{S}'_1 \hat{V}_1^\text{T} Z_1) r_1 + \sigma_{W1} \hat{W}_1] \quad (70)$$

$$\dot{\hat{V}}_1 = -\Gamma_{V1} [Z_1 \hat{W}_1^\text{T} \hat{S}'_1 r_1 + \sigma_{V1} \hat{V}_1] \quad (71)$$

where $k_1 > 0$, $\delta_1 > 0$, $\Gamma_{W1} = \Gamma_{W1}^\text{T} > 0$, $\Gamma_{V1} = \Gamma_{V1}^\text{T} > 0$, $\sigma_{W1} > 0$, $\sigma_{V1} > 0$.

Substituting (69)–(71) in (68), we have

$$\begin{aligned} \dot{V}_1 &= -k_1 b_{11}(\dot{q}_3) r_1^2 - \frac{b_{11}(\dot{q}_3)}{\hat{b}_{11}} \frac{r_1^2 (\hat{W}_1^\text{T} S(\hat{V}_1^\text{T} Z_1))^2}{(|r_1 \hat{W}_1^\text{T} S(\hat{V}_1^\text{T} Z_1)| + \delta_1)} \\ &- \frac{b_{11}(\dot{q}_3)}{\hat{b}_{11}} k_1 r_1^2 (\|Z_1 \hat{W}_1^\text{T} \hat{S}'_1\|_F^2 + \|\hat{S}'_1 \hat{V}_1^\text{T} Z_1\|^2) \\ &- r_1 W_1^{*\text{T}} S_1(V_1^{*\text{T}} Z_1) - r_1 \varepsilon_1(Z_1) - r_1 \tilde{W}_1^\text{T} (\hat{S}_1 - \hat{S}'_1 \hat{V}_1^\text{T} Z_1) \\ &- \sigma_{W1} \tilde{W}_1^\text{T} \hat{W}_1 - \text{tr} \{ \tilde{V}_1^\text{T} Z_1 \hat{W}_1^\text{T} \hat{S}'_1 r_1 \} - \sigma_{V1} \text{tr} \{ \tilde{V}_1^\text{T} \hat{V}_1 \} \end{aligned} \quad (72)$$

Noting Assumption 3 and the fact that $\text{tr} \{ \tilde{V}_1^\text{T} Z_1 \hat{W}_1^\text{T} \hat{S}'_1 r_1 \} = r_1 \hat{W}_1^\text{T} \hat{S}'_1 \tilde{V}_1^\text{T} Z_1$, (72) becomes

$$\begin{aligned} \dot{V}_1 &\leq -k_1 \hat{b}_{11} r_1^2 - \frac{r_1^2 (\hat{W}_1^\text{T} S(\hat{V}_1^\text{T} Z_1))^2}{(|r_1 \hat{W}_1^\text{T} S(\hat{V}_1^\text{T} Z_1)| + \delta_1)} \\ &- k_1 r_1^2 (\|Z_1 \hat{W}_1^\text{T} \hat{S}'_1\|_F^2 + \|\hat{S}'_1 \hat{V}_1^\text{T} Z_1\|^2) + |r_1| |\varepsilon_1(Z_1)| \\ &- r_1 W_1^{*\text{T}} S_1(V_1^{*\text{T}} Z_1) - r_1 \tilde{W}_1^\text{T} (\hat{S}_1 - \hat{S}'_1 \hat{V}_1^\text{T} Z_1) \\ &- r_1 \hat{W}_1^\text{T} \hat{S}'_1 \tilde{V}_1^\text{T} Z_1 - \sigma_{W1} \tilde{W}_1^\text{T} \hat{W}_1 - \sigma_{V1} \text{tr} \{ \tilde{V}_1^\text{T} \hat{V}_1 \} \end{aligned} \quad (73)$$

From (63) and (64), we know

$$\begin{aligned} & -r_1 W_1^{*\text{T}} S_1(V_1^{*\text{T}} Z_1) - r_1 \tilde{W}_1^\text{T} (\hat{S}_1 - \hat{S}'_1 \hat{V}_1^\text{T} Z_1) - r_1 \hat{W}_1^\text{T} \hat{S}'_1 \tilde{V}_1^\text{T} Z_1 \\ &= -r_1 \hat{W}_1^\text{T} S(\hat{V}_1^\text{T} Z_1) - r_1 d_{u1} \\ &\leq |r_1| \hat{W}_1^\text{T} S(\hat{V}_1^\text{T} Z_1) + |r_1| \|W_1^*\|_F \|Z_1\| \hat{W}_1^\text{T} \hat{S}'_1 \|Z_1\| \\ &+ |r_1| \|W_1^*\| \|\hat{S}'_1 \hat{V}_1^\text{T} Z_1\| + |r_1| |W_1^*|_1 \end{aligned} \quad (74)$$

Substituting (74) into (73) leads to

$$\begin{aligned} \dot{V}_1 \leq & -k_1 b_{11} r_1^2 - \frac{r_1^2 (\hat{W}_1^T S(\hat{V}_1^T Z_1))^2}{(|r_1 \hat{W}_1^T S(\hat{V}_1^T Z_1)| + \delta_1)} + |r_1 \hat{W}_1^T S(\hat{V}_1^T Z_1)| \\ & - k_1 r_1^2 (\|Z_1 \hat{W}_1^T \hat{S}'_1\|_F^2 + \|\hat{S}'_1 \hat{V}_1^T Z_1\|^2) + |r_1| |\varepsilon_1(Z_1)| \\ & + |r_1| \|V_1^*\|_F \|Z_1 \hat{W}_1^T \hat{S}'_1\|_F + |r_1| \|W_1^*\| \|\hat{S}'_1 \hat{V}_1^T Z_1\| \\ & + |r_1| \|W_1^*\|_1 - \sigma_{W1} \tilde{W}_1^T \hat{W}_1 - \sigma_{V1} \text{tr}\{\tilde{V}_1^T \hat{V}_1\} \end{aligned} \quad (75)$$

According to Lemma 1,

$$\begin{aligned} & - \frac{r_1^2 (\hat{W}_1^T S(\hat{V}_1^T Z_1))^2}{|r_1 \hat{W}_1^T S(\hat{V}_1^T Z_1)| + \delta_1} + |r_1 \hat{W}_1^T S(\hat{V}_1^T Z_1)| \\ & = \frac{|r_1 \hat{W}_1^T S(\hat{V}_1^T Z_1)| \delta_1}{|r_1 \hat{W}_1^T S(\hat{V}_1^T Z_1)| + \delta_1} \leq \delta_1 \end{aligned} \quad (76)$$

By completion of squares and using Young's inequality, the following inequalities hold

$$|r_1| |\varepsilon_1(Z_1)| \leq \frac{r_1^2}{2c_{11}} + \frac{c_{11} \bar{\varepsilon}_1^2}{2} \quad (77)$$

$$|r_1| \|V_1^*\|_F \|Z_1 \hat{W}_1^T \hat{S}'_1\|_F \leq k_1 r_1^2 \|Z_1 \hat{W}_1^T \hat{S}'_1\|_F^2 + \frac{1}{4k_1} \|V_1^*\|_F^2 \quad (78)$$

$$|r_1| \|W_1^*\| \|\hat{S}'_1 \hat{V}_1^T Z_1\| \leq k_1 r_1^2 \|\hat{S}'_1 \hat{V}_1^T Z_1\|^2 + \frac{1}{4k_1} \|W_1^*\|^2 \quad (79)$$

$$|r_1| \|W_1^*\|_1 \leq \frac{r_1^2}{2c_{12}} + \frac{c_{12} \|W_1^*\|_1^2}{2} \quad (80)$$

$$-\sigma_{W1} \tilde{W}_1^T \hat{W}_1 \leq -\frac{\sigma_{W1}}{2} \|\tilde{W}_1\|^2 + \frac{\sigma_{W1}}{2} \|W_1^*\|^2 \quad (81)$$

$$-\sigma_{V1} \text{tr}\{\tilde{V}_1^T \hat{V}_1\} \leq -\frac{\sigma_{V1}}{2} \|\tilde{V}_1\|_F^2 + \frac{\sigma_{V1}}{2} \|V_1^*\|_F^2 \quad (82)$$

Substituting (76)–(82) into (85), we have

$$\begin{aligned} \dot{V}_1 \leq & - \left(k_1 b_{11} - \frac{1}{2c_{11}} - \frac{1}{2c_{12}} \right) r_1^2 - \frac{\sigma_{W1}}{2} \|\tilde{W}_1\|^2 \\ & - \frac{\sigma_{V1}}{2} \|\tilde{V}_1\|_F^2 + \delta_1 + \left(\frac{\sigma_{W1}}{2} + \frac{1}{4k_1} \right) \|W_1^*\|^2 \\ & + \left(\frac{\sigma_{V1}}{2} + \frac{1}{4k_1} \right) \|V_1^*\|_F^2 + \frac{c_{11}}{2} \bar{\varepsilon}_1^2 + \frac{c_{12} \|W_1^*\|_1^2}{2} \\ & \leq -\lambda_{10} V_1 + \mu_{10} \end{aligned} \quad (83)$$

where $\lambda_{10} = \min\{(2k_1 b_{11} - 1/c_{11} - 1/c_{12})/d_{11}, \sigma_{W1}/\lambda_{\max}(\Gamma_{W1}^{-1}), \sigma_{V1}/\lambda_{\max}(\Gamma_{V1}^{-1})\}$, $\mu_{10} = \delta_1 + (\sigma_{W1}/2 + 1/4k_1) \|W_1^*\|^2 + (\sigma_{V1}/2 + 1/4k_1) \|V_1^*\|_F^2 + (c_{11}/2) \bar{\varepsilon}_1^2 + (c_{12} \|W_1^*\|_1^2)/2$.

3.2.2 q_2 subsystem: Similar to Section 3.1.2, (10) becomes

$$\frac{d_{22}(q_3)d_{33} - d_{23}^2}{d_{33}} \dot{r}_2 + c_{22}(q_3, \dot{q}_3)r_2 = b_{22}(\dot{q}_3)\tau_2 - f_{s2,1} \quad (84)$$

where the unknown function

$$\begin{aligned} f_{s2,1} = & \frac{d_{22}(q_3)d_{33} - d_{23}^2}{d_{33}} \dot{q}_{2r} + c_{22}(q_3, \dot{q}_3)\dot{q}_{2r} \\ & + c_{23}(q_3, \dot{q}_2)\dot{q}_3 + \Delta_2(q, \dot{q}) + \frac{d_{23}}{d_{33}}(b_{31}(\dot{q}_3)\tau_1 \\ & - c_{32}(q_3, \dot{q}_2)\dot{q}_2 - f_3(\dot{q}_3) - g_3 - \Delta_3(q, \dot{q})) \end{aligned}$$

is approximated by MNN to arbitrary any accuracy as

$$f_{s2,1} = W_2^{*\Gamma} S_2(V_2^{*\Gamma} Z_2) + \varepsilon_2(Z_2)$$

where the input vector $Z_2 = [\tau_1, q_1, \dot{q}_1, q_2, \dot{q}_2, q_3, \dot{q}_3, q_{2d}, \dot{q}_{2d}, \ddot{q}_{2d}, 1]^T \in \Omega_{Z_2} \subset R^{11}$, $\varepsilon_2(Z_2)$ is the approximation error satisfying $|\varepsilon_2(Z_2)| \leq \bar{\varepsilon}_2$, where $\bar{\varepsilon}_2$ is a positive constant; W_2^* and V_2^* are ideal constant weights satisfying $\|W_2^*\| \leq w_{2m}$, $\|V_2^*\|_F \leq v_{2m}$, which are positive constants. By using $\hat{W}_2^T S_2(\hat{V}_2^T Z_2)$ to approximate $W_2^{*\Gamma} S_2(V_2^{*\Gamma} Z_2)$, the error between the actual and the ideal MNN can be expressed as

$$\begin{aligned} & \hat{W}_2^T S(\hat{V}_2^T Z_2) - W_2^{*\Gamma} S(V_2^{*\Gamma} Z_2) \\ & = \tilde{W}_2^T (\hat{S}_2 - \hat{S}'_2 \hat{V}_2^T Z_2) + \hat{W}_2^T \hat{S}'_2 \tilde{V}_2^T Z_2 + d_{u2} \end{aligned} \quad (85)$$

where $\hat{S}_2 = S(\hat{V}_2^T Z_2)$, $\hat{S}'_2 = \text{diag}\{\hat{s}'_1, \hat{s}'_2, \dots, \hat{s}'_i\}$ with

$$\hat{s}'_i = s'(\hat{v}_i^T Z_2) = \left. \frac{d[s(z_a)]}{dz_a} \right|_{z_a = \hat{v}_i^T Z_2}$$

the residual term d_{u2} is bounded by

$$|d_{u2}| \leq \|V_2^*\|_F \|Z_2 \hat{W}_2^T \hat{S}'_2\|_F + \|W_2^*\| \|\hat{S}'_2 \hat{V}_2^T Z_2\| + \|W_2^*\|_1 \quad (86)$$

and the weight estimation errors $\tilde{W}_2 = \hat{W}_2 - W_2^*$, $\tilde{V}_2 = \hat{V}_2 - V_2^*$.

To analyse the closed-loop stability for the q_2 -subsystem, consider the following Lyapunov function candidate

$$\begin{aligned} V_2(r_2, \tilde{W}_2, \tilde{V}_2) = & \frac{1}{2} \frac{d_{22}(q_3)d_{33} - d_{23}^2}{d_{33}} r_2^2 \\ & + \frac{1}{2} \tilde{W}_2^T \Gamma_{W2}^{-1} \tilde{W}_2 + \frac{1}{2} \text{tr}\{\tilde{V}_2^T \Gamma_{V2}^{-1} \tilde{V}_2\} \end{aligned} \quad (87)$$

Lemma 5: The function V_2 (87) is positive definite and decrescent, in the sense that there exist two time-invariant positive definite functions $\underline{V}_2(r_2, \tilde{W}_2, \tilde{V}_2)$ and $\bar{V}_2(r_2, \tilde{W}_2, \tilde{V}_2)$, such that

$$\underline{V}_2(r_2, \tilde{W}_2, \tilde{V}_2) \leq V_2 \leq \bar{V}_2(r_2, \tilde{W}_2, \tilde{V}_2)$$

Proof: The proof can be referred to that of Lemma 3 and omitted here for conciseness. \square

The time derivative of (87) is given as

$$\begin{aligned} \dot{V}_2 = & \frac{1}{2} \dot{d}_{22}(q_3)r_2^2 + \frac{d_{22}(q_3)d_{33} - d_{23}^2}{d_{33}} r_2 \dot{r}_2 \\ & + \tilde{W}_2^T \Gamma_2^{-1} \dot{\tilde{W}}_2 + \text{tr}\{\tilde{V}_2^T \Gamma_{V_2}^{-1} \dot{\tilde{V}}_2\} \end{aligned} \quad (88)$$

According to Assumption 2, (88) becomes

$$\begin{aligned} \dot{V}_2 = & r_2 \left[\frac{d_{22}(q_3)d_{33} - d_{23}^2}{d_{33}} \dot{r}_2 + c_{22}(q_3, \dot{q}_3)r_2 \right] \\ & + \tilde{W}_2^T \Gamma_2^{-1} \dot{\tilde{W}}_2 + \text{tr}\{\tilde{V}_2^T \Gamma_{V_2}^{-1} \dot{\tilde{V}}_2\} \end{aligned} \quad (89)$$

As W_2^* , V_2^* are constant vectors, it is easy to obtain that

$$\dot{\tilde{W}}_2 = \dot{W}_2, \quad \dot{\tilde{V}}_2 = \dot{V}_2 \quad (90)$$

Substituting (84), (85) and (90) into (94), we have

$$\begin{aligned} \dot{V}_2 = & r_2 \left[b_{22}(\dot{q}_3)\tau_2 - W_2^{*T} S_2(V_2^{*T} Z_2) - \varepsilon_2(Z_2) \right] \\ & + \tilde{W}_2^T \Gamma_{W_2}^{-1} \dot{\tilde{W}}_2 + \text{tr}\{\tilde{V}_2^T \Gamma_{V_2}^{-1} \dot{\tilde{V}}_2\} \end{aligned} \quad (91)$$

Consider the following MNN-based control law and MNN weight adaption laws

$$\begin{aligned} \tau_2 = & k_2 r_2 + \frac{r_2 \left(\hat{W}_2^T S(\hat{V}_2^T Z_2) \right)^2}{\underline{b}_{22} \left(|r_2 \hat{W}_2^T S(\hat{V}_2^T Z_2)| + \delta_2 \right)} \\ & + \frac{k_2 r_2}{\underline{b}_{22}} \left(\|Z_2 \hat{W}_2^T \hat{S}'_2\|_F^2 + \|\hat{S}'_2 \hat{V}_2^T Z_2\|^2 \right) \end{aligned} \quad (92)$$

$$\dot{\hat{W}}_2 = -\Gamma_{W_2} [(\hat{S}_2 - \hat{S}'_2 \hat{V}_2^T Z_2)r_2 + \sigma_{W_2} \hat{W}_2] \quad (93)$$

$$\dot{\hat{V}}_2 = -\Gamma_{V_2} [Z_2 \hat{W}_2^T \hat{S}'_2 r_2 + \sigma_{V_2} \hat{V}_2] \quad (94)$$

where $k_2 > 0$, $\delta_2 > 0$, $\Gamma_{W_2} = \Gamma_{W_2}^T > 0$, $\Gamma_{V_2} = \Gamma_{V_2}^T > 0$, $\sigma_{W_2} > 0$, $\sigma_{V_2} > 0$.

Substituting (92)–(94) into (91), we have

$$\begin{aligned} \dot{V}_2 = & k_2 b_{22}(\dot{q}_3)r_2^2 + \frac{b_{22}(\dot{q}_3)}{\underline{b}_{22}} \frac{r_2^2 \left(\hat{W}_2^T S(\hat{V}_2^T Z_2) \right)^2}{\left(|r_2 \hat{W}_2^T S(\hat{V}_2^T Z_2)| + \delta_2 \right)} \\ & + \frac{b_{22}(\dot{q}_3)}{\underline{b}_{22}} k_2 r_2^2 \left(\|Z_2 \hat{W}_2^T \hat{S}'_2\|_F^2 + \|\hat{S}'_2 \hat{V}_2^T Z_2\|^2 \right) \\ & - r_2 W_2^{*T} S_2(V_2^{*T} Z_2) - r_2 \varepsilon_2(Z_2) - r_2 \tilde{W}_2^T (\hat{S}_2 - \hat{S}'_2 \hat{V}_2^T Z_2) \\ & - \sigma_{W_2} \tilde{W}_2^T \hat{W}_2 - \text{tr}\{\tilde{V}_2^T Z_2 \hat{W}_2^T \hat{S}'_2 r_2\} - \sigma_{V_2} \text{tr}\{\tilde{V}_2^T \hat{V}_2\} \end{aligned} \quad (95)$$

Noting Assumption 3 and the fact that $\text{tr}\{\tilde{V}_2^T Z_2 \hat{W}_2^T \hat{S}'_2 r_2\} = r_2 \hat{W}_2^T \hat{S}'_2 \tilde{V}_2^T Z_2$, (95) becomes

$$\begin{aligned} \dot{V}_2 \leq & -k_2 \underline{b}_{22} r_1^2 - \frac{r_2^2 \left(\hat{W}_2^T S(\hat{V}_2^T Z_2) \right)^2}{\left(|r_2 \hat{W}_2^T S(\hat{V}_2^T Z_2)| + \delta_2 \right)} \\ & - k_2 r_2^2 \left(\|Z_2 \hat{W}_2^T \hat{S}'_2\|_F^2 + \|\hat{S}'_2 \hat{V}_2^T Z_2\|^2 \right) + |r_2| \varepsilon_2(Z_2) \\ & - r_2 W_2^{*T} S_2(V_2^{*T} Z_2) - r_2 \tilde{W}_2^T (\hat{S}_2 - \hat{S}'_2 \hat{V}_2^T Z_2) \\ & - r_2 \hat{W}_2^T \hat{S}'_2 \tilde{V}_2^T Z_2 - \sigma_{W_2} \tilde{W}_2^T \hat{W}_2 - \sigma_{V_2} \text{tr}\{\tilde{V}_2^T \hat{V}_2\} \end{aligned} \quad (96)$$

From (85) and (86), we know

$$\begin{aligned} & -r_2 W_2^{*T} S_2(V_2^{*T} Z_2) - r_2 \tilde{W}_2^T (\hat{S}_2 - \hat{S}'_2 \hat{V}_2^T Z_2) - r_2 \hat{W}_2^T \hat{S}'_2 \tilde{V}_2^T Z_2 \\ & = -r_2 \hat{W}_2^T S(\hat{V}_2^T Z_2) - r_2 d_{u2} \\ & \leq |r_2| \hat{W}_2^T S(\hat{V}_2^T Z_2) + |r_2| \|V_2^*\|_F \|Z_2 \hat{W}_2^T \hat{S}'_2\|_F \\ & \quad + |r_2| \|W_2^*\| \|\hat{S}'_2 \hat{V}_2^T Z_2\| + |r_2| \|W_2^*\|_1 \end{aligned} \quad (97)$$

Substituting (97) to (96) leads to

$$\begin{aligned} \dot{V}_2 \leq & -k_2 \underline{b}_{22} r_2^2 - \frac{r_2^2 \left(\hat{W}_2^T S(\hat{V}_2^T Z_2) \right)^2}{\left(|r_2 \hat{W}_2^T S(\hat{V}_2^T Z_2)| + \delta_2 \right)} + |r_2| \hat{W}_2^T S(\hat{V}_2^T Z_2) \\ & - k_2 r_2^2 \left(\|Z_2 \hat{W}_2^T \hat{S}'_2\|_F^2 + \|\hat{S}'_2 \hat{V}_2^T Z_2\|^2 \right) \\ & + |r_2| \varepsilon_2(Z_2) + |r_2| \|V_2^*\|_F \|Z_2 \hat{W}_2^T \hat{S}'_2\|_F \\ & + |r_2| \|W_2^*\| \|\hat{S}'_2 \hat{V}_2^T Z_2\| + |r_2| \|W_2^*\|_1 \\ & - \sigma_{W_2} \tilde{W}_2^T \hat{W}_2 - \sigma_{V_2} \text{tr}\{\tilde{V}_2^T \hat{V}_2\} \end{aligned} \quad (98)$$

According to Lemma 1

$$\begin{aligned} & - \frac{r_2^2 \left(\hat{W}_2^T S(\hat{V}_2^T Z_2) \right)^2}{\left(|r_2 \hat{W}_2^T S(\hat{V}_2^T Z_2)| + \delta_2 \right)} + |r_2| \hat{W}_2^T S(\hat{V}_2^T Z_2) \\ & = \frac{|r_2| \hat{W}_2^T S(\hat{V}_2^T Z_2) \delta_2}{|r_2| \hat{W}_2^T S(\hat{V}_2^T Z_2) + \delta_2} \leq \delta_2 \end{aligned} \quad (99)$$

By completion of squares and using Young's inequality, the following inequalities hold

$$|r_2| \varepsilon_2(Z_2) \leq \frac{r_2^2}{2c_{21}} + \frac{c_{21} \bar{\varepsilon}_2^2}{2} \quad (100)$$

$$|r_2| \|V_2^*\|_F \|Z_2 \hat{W}_2^T \hat{S}'_2\|_F \leq k_2 r_2^2 \|Z_2 \hat{W}_2^T \hat{S}'_2\|_F^2 + \frac{1}{4k_2} \|V_2^*\|_F^2 \quad (101)$$

$$|r_2| \|W_2^*\| \|\hat{S}_2' \hat{V}_2^T Z_2\| \leq k_2 r_2^2 \|\hat{S}_2' \hat{V}_2^T Z_2\|^2 + \frac{1}{4k_2} \|W_2^*\|^2 \quad (102)$$

$$|r_2| \|W_2^*\|_1 \leq \frac{r_2^2}{2c_{22}} + \frac{c_{22} \|W_2^*\|_1^2}{2} \quad (103)$$

$$-\sigma_{W_2} \tilde{W}_2^T \hat{W}_2 \leq -\frac{\sigma_{W_2}}{2} \|\tilde{W}_2\|^2 + \frac{\sigma_{W_2}}{2} \|W_1^*\|^2 \quad (104)$$

$$-\sigma_{V_2} \text{tr}\{\tilde{V}_2^T \hat{V}_2\} \leq -\frac{\sigma_{V_2}}{2} \|\tilde{V}_2\|_F^2 + \frac{\sigma_{V_2}}{2} \|V_2^*\|_F^2 \quad (105)$$

Substituting (99)–(105) into (98), we have

$$\begin{aligned} \dot{V}_2 \leq & -\left(k_2 b_{22} - \frac{1}{2c_{21}} - \frac{1}{2c_{22}}\right) r_2^2 - \frac{\sigma_{W_2}}{2} \|\tilde{W}_2\|^2 \\ & - \frac{\sigma_{V_2}}{2} \|\tilde{V}_2\|_F^2 + \delta_2 + \left(\frac{\sigma_{W_2}}{2} + \frac{1}{4k_2}\right) \|W_2^*\|^2 \\ & + \left(\frac{\sigma_{V_2}}{2} + \frac{1}{4k_2}\right) \|V_2^*\|_F^2 + \frac{c_{21}}{2} \bar{\epsilon}_2^2 + \frac{c_{22} \|W_2^*\|_1^2}{2} \\ \leq & -\lambda_{20} V_2 + \mu_{20} \end{aligned} \quad (106)$$

where $\lambda_{20} = \min\{(2k_2 b_{22} - 1/c_{21} - 1/c_{22})|d_{33}|/(\bar{d}_{22}|d_{33}| + d_{23}^2), \sigma_{W_2}/\lambda_{\max}(\Gamma_{W_2}^{-1}), \sigma_{V_2}/\lambda_{\max}(\Gamma_{V_2}^{-1})\}$, $\mu_{20} = \delta_2 + (\sigma_{W_2}/2 + 1/4k_2)\|W_2^*\|^2 + (\sigma_{V_2}/2 + 1/4k_2)\|V_2^*\|_F^2 + (c_{21}/2)\bar{\epsilon}_2^2 + c_{22}\|W_2^*\|_1^2/2$.

3.2.3 q_3 subsystem: Finally, for the system (9)–(11) under control laws (69), (92), we can obtain the similar internal dynamics to Section 3.1.3.

The main result in this section is summarised in the following Theorem.

Theorem 2: Consider the closed-loop system consisting of the subsystems (9)–(11), the control laws (69), (92), and adaptation laws (70), (71), (93) and (94). Under Assumptions 1–8, the overall closed-loop neural control system is SGUUB in the sense that all of the signals in the closed-loop system are bounded, and the tracking errors and weights converge to the following regions

$$|e_1| \leq |e_1(0)| + \frac{1}{\lambda_1} \sqrt{\frac{2\mu_1}{d_{11}}}, \|\hat{W}_1\| \leq \sqrt{\frac{2\mu_1}{\lambda_{\min}(\Gamma_1^{-1})}} + w_{1m}$$

$$\|\hat{V}_1\|_F \leq \sqrt{\frac{2\mu_1}{\lambda_{\min}(\Gamma_1^{-1})}} + v_{1m}$$

$$|e_2| \leq |e_2(0)| + \frac{1}{\lambda_2} \sqrt{\frac{2|d_{33}|\mu_2}{|\bar{d}_{22}|d_{33}| - d_{23}^2}}$$

$$\|\hat{W}_2\| \leq \sqrt{\frac{2\mu_2}{\lambda_{\min}(\Gamma_2^{-1})}} + w_{2m}, \|\hat{V}_2\| \leq \sqrt{\frac{2\mu_2}{\lambda_{\min}(\Gamma_2^{-1})}} + v_{2m}$$

with

$$\mu_i = \frac{\mu_{i0}}{\lambda_{i0}} + V_i(0)$$

$$\begin{aligned} \mu_{i0} = & \delta_i + \left(\frac{\sigma_{W_i}}{2} + \frac{1}{4k_i}\right) \|W_i^*\|^2 + \left(\frac{\sigma_{V_i}}{2} + \frac{1}{4k_{i1}}\right) \|V_i^*\|_F^2 \\ & + \frac{c_{i1}}{2} \bar{\epsilon}_i^2 + \frac{c_{i2} \|W_i^*\|_1^2}{2}, \quad i = 1, 2 \end{aligned}$$

$$\lambda_{10} = \min\{(2k_1 b_{11} - 1/c_{11} - 1/c_{12})/d_{11}$$

$$\sigma_{W_1}/\lambda_{\max}(\Gamma_{W_1}^{-1}), \sigma_{V_1}/\lambda_{\max}(\Gamma_{V_1}^{-1})\}$$

$$\lambda_{20} = \min\{(2k_2 b_{22} - 1/c_{21} - 1/c_{22})|d_{33}|/(\bar{d}_{22}|d_{33}| + d_{23}^2)$$

$$\sigma_{W_2}/\lambda_{\max}(\Gamma_{W_2}^{-1}), \sigma_{V_2}/\lambda_{\max}(\Gamma_{V_2}^{-1})\}$$

where $e_i(0)$ and $V_i(0)$ are initial values of $e_i(t)$ and $V_i(t)$, respectively.

Proof: The proof of Theorem 2 follows the same approach as Theorem 1, and is omitted here for conciseness. \square

4 Simulation study

To illustrate the proposed adaptive neural control, we consider the VARIO helicopter mounted on a platform [6], with the dynamic model as (2) and the following parameters $d_{11} = 7.5$, $d_{22}(q_3) = 0.4305 + 0.0003\cos^2(-4.143q_3)$, $d_{23} = 0.108$, $d_{33} = 0.4993$, $c_{22}(q_3, \dot{q}_3) = 0.0006214 \sin(-8.286q_3)\dot{q}_3$, $c_{23}(q_3, \dot{q}_2) = c_{32}(q_3, \dot{q}_2) = 0.0006214 \sin(-8.286q_3)\dot{q}_2$, $f_1(\dot{q}_3) = -0.6004\dot{q}_3$, $f_3(\dot{q}_3) = -0.0001206\dot{q}_3^2$, $g_1 = -77.259$, $g_3 = -2.642$, $b_{11}(\dot{q}_3) = 3.411\dot{q}_3^2$, $b_{22}(\dot{q}_3) = -0.1525\dot{q}_3^2$, $b_{31}(\dot{q}_3) = 12.01\dot{q}_3 + 10^5$, and all quantities are expressed in SI units. The control objective is to track the uniformly bounded desired trajectories given in [6] as follows

$$q_{1d} = \begin{cases} -0.2 & 0 \leq t \leq 50s \\ 0.3[e^{-(t-50)^2/350} - 1] - 0.2 & 50 < t \leq 130s \\ 0.1 \cos[(t-130)/10] - 0.6 & 130 < t \leq 20\pi + 130 \\ -0.5 & t \geq 20\pi + 130 \end{cases}$$

$$q_{2d} = \begin{cases} 0 & t < 50s \\ 1 - e^{-(t-50)^2/350} & 50 \leq t < 120s \\ e^{-(t-120)^2/350} & 120 \leq t < 180 \\ -1 + e^{-(t-180)^2/350} & t \geq 180 \end{cases}$$

4.1 Internal dynamics stability analysis

In this section, we analyse the stability of the internal dynamics. For conciseness, we consider the RBFNN-based control case only, which can be easily extended to MNN-based control case without any difficulties. For the RBFNN based control case, we substitute (15), (20), (30) and (38) into the q_3 -subsystem (11). According to the definition of the zero-dynamics [26], we set r_1, r_2, \tilde{W}_1^T ,

\tilde{W}_2^T , $\varepsilon_1(Z_1)$ and $\varepsilon_2(Z_2)$ to zero, and that the desired trajectories and initial data can be chosen in such a way that terms including \dot{q}_2^2 , \ddot{q}_{1d} , \ddot{q}_{2d} can be neglected [6], we have

$$\ddot{q}_3 = \frac{1}{d_{33}} \left[\frac{b_{31}(\dot{q}_3)}{b_{11}(\dot{q}_3)} (f_1(\dot{q}_3) + g_1) - f_3(\dot{q}_3) - g_3 \right] \quad (107)$$

Noticing that the zero-dynamics in (107) is nonlinear, it is difficult to conduct the stability analysis of the nonlinear zero-dynamics directly in this example. Instead, we show its local stability within an interested operating region after linearising the nonlinear zero-dynamics around an equilibrium operating point of interest. Although the stability of the linearised system cannot exactly guarantee the stability of the nonlinear zero-dynamics, the local stability is at least ensured within the operating region of interest. To realise this, we need to solve for the equilibrium points first.

Substituting the term values given in the beginning of Section 4 into (107) and analysing the values of the main rotor angular velocity from which the main rotor angular acceleration is zero, we have

$$4.1137 \times 10^{-4} \dot{q}_3^4 + 1.8011 \dot{q}_3^2 - 60968 \dot{q}_3 - 7725900 = 0 \quad (108)$$

Its solutions are $\dot{q}_3^* = -124.63$, $-219.5 \pm 468.16i$ and 563.64 rad/s. Only the first value $\dot{q}_3^* = -124.63$ has a physical meaning for the system (see Fig. 1 for the rotation sense of the main rotor). If we linearise equation (107) around the equilibrium point $\dot{q}_3^* = -124.63$, we can obtain an eigenvalue -2.44 . Therefore according to [27], all initial values of \dot{q}_3 sufficiently near the equilibrium point $\dot{q}_3^* = -124.63$ can converge to -124.63 , indicating that the zero-dynamics of the helicopter system in (2) has a locally stable behaviour around the equilibrium point. The limitation of this analysis is that if the initial conditions are far from the operating region of interest, the stability of the zero-dynamics is not guaranteed.

The simulation result in Fig. 2 also shows that the zero-dynamics using RBFNN-based control are locally stable around the equilibrium point $\dot{q}_3^* = -124.63$. From Fig. 2, we can observe that the main rotor angular velocity \dot{q}_3 converges to the nominal value -124.63 rad/s for different initial conditions ranging from -40 to -150 rad/s, which includes the typical operating values more than sufficiently. These results are expected from the previous stability analysis, and also consistent with the results in [6]. In particular, we also notice that the further the initial condition starts from the nominal value -124.63 rad/s, the longer the settling time takes, and the more seriously the transient oscillations become.

4.2 Performance comparison results between approximation-based control and model-based control

In this subsection, we will compare the altitude and yaw angle tracking performance using RBFNN-based control, MNN-based control and model-based control adopted in [6]. If all the parameters and functions in (2) are known exactly, and the unmodelled uncertainties $\Delta(\cdot) = 0$, the perfect tracking performance can be achieved using model-based control, which has been shown in the work [6]. However, in the practice, there always exist some model uncertainties, which may be caused by unmodelled dynamics or aerodynamical disturbances from the environment. To this end, we assume $\Delta(\cdot) \neq 0$, in particular, $\Delta(\cdot) = [2.0, 0, 0.0001206\dot{q}_3^2 + 0.142]^T$.

The control parameters for the RBFNN control laws (20) (38) and adaptation laws (21) (39) are chosen as follows: $k_1 = 0.000085$, $\Lambda_1 = 0.2$, $k_2 = 0.0002$, $\Lambda_2 = 1.0$, $\Gamma_1 = 0.001I$, $\Gamma_2 = 0.0001I$, $\sigma_1 = 0.001$, $\sigma_2 = 0.001$. NNs $\hat{W}_1^T S_1(Z_1)$ contain 3^8 nodes (i.e. $l_1 = 2187$), with centres $\mu_l (l = 1, \dots, l_1)$ evenly spaced in $[-1.0, 1.0] \times [-0.1, 0.1] \times [-10.0, -10.0] \times [-40000.0, 0.0] \times [-1.0, 1.0] \times [-150.0, -40.0] \times [-0.1, 0.1] \times [-0.01, 0.01]$, and widths $\eta_l (l = 1, \dots, l_1)$. NNs $\hat{W}_2^T S_2(Z_2)$ contain 3^{10} nodes (i.e. $l_2 = 59049$), with centres $\mu_l (l = 1, \dots, l_2)$ evenly spaced in $[-0.005, 0.005] \times [-1.0, 1.0] \times [-0.1, 0.1] \times [-10.0, -10.0] \times [-40000.0, 0.0] \times [-1.0, 1.0] \times [-150.0, -40.0] \times [-10.0, 10.0] \times [-1.0, 1.0] \times [-0.01, 0.01]$, and widths $\eta_l (l = 1, \dots, l_2)$. The initial conditions are $q_1(0) = 0.1$ m, $\dot{q}_1(0) = 0.0$ m/s, $q_2(0) = -\pi$ rad, $\dot{q}_2(0) = 0.0$ rad/s, $q_3(0) = -\pi$ rad, $\dot{q}_3(0) = -120.0$ rad/s, $\tau_1 = 0.0$ m, $\tau_2 = 0.0$ m, $\tilde{W}_1(0) = 0.0$, $\tilde{W}_2(0) = 0.0$.

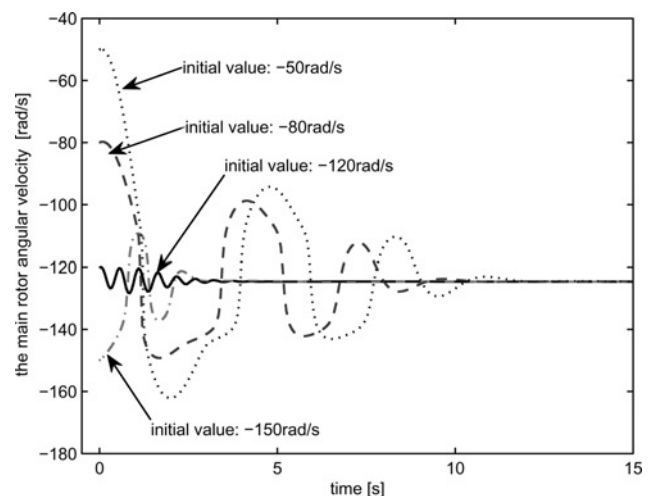


Figure 2 Local stability of the zero-dynamics around the equilibrium point $\dot{q}_3^* = -124.63$ using RBFNN-based control

For the MNN control laws (69) and (92) and adaptation laws (70), (71), (93) and (94), the design parameters are chosen as $k_1 = 0.00016$, $\Lambda_1 = 1.2$, $k_2 = 0.0002$, $\Lambda_2 = 1.0$, $\Gamma_{W1} = 0.0002I$, $\Gamma_{V1} = 0.03I$, $\delta_{W1} = 0.0$, $\sigma_{V1} = 0.0$, $\Gamma_{W2} = 0.0001I$, $\Gamma_{V2} = 0.01I$, $\sigma_{W2} = 0.0$, $\sigma_{V2} = 0.0$. NNs $\hat{W}_1^T S_1(\hat{V}_1^T \tilde{z}_1)$ contain five nodes and NNs $\hat{W}_2^T S_2(\hat{V}_2^T \tilde{z}_2)$ contains 15 nodes. The initial conditions are $q_1(0) = 0.1$ m, $\dot{q}_1(0) = 0$ m/s, $q_2(0) = -\pi$ rad, $\dot{q}_2(0) = 0.0$ rad/s, $q_3(0) = -\pi$ rad, $\dot{q}_3(0) = -120.0$ rad/s, $\tau_1 =$

0.0 m, $\tau_2 = 0.0$ m, $\hat{W}_1(0) = 0.0$, $\hat{V}_1(0) = 0.0$, $\hat{W}_2(0) = 0.0$, $\hat{V}_2(0) = 0.0$.

From Figs. 3 and 4, we can observe that due to the existence of model uncertainties, both the altitude tracking and yaw angle tracking using model-based control have some offsets to the desired trajectories for the whole period. It means that model-based control depends on the accuracy of model heavily and cannot deal with the uncertainties well. For the tracking performance using the RBFNN-based control and MNN-based control, although there are also some oscillations at the beginning period, the tracking errors can converge to a very small neighbourhood of desired

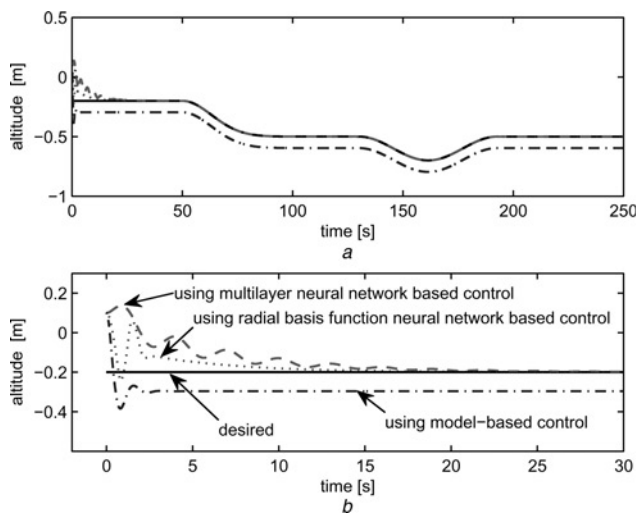


Figure 3 Altitude tracking performance in the presence of model uncertainties using three methods: RBFNN-based control, MNN-based control and model-based control, respectively

a Zoom-out
b Zoom-in

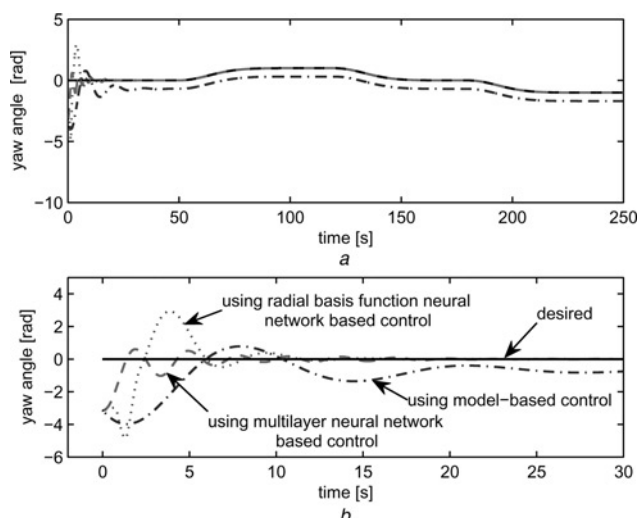


Figure 4 Yaw angle tracking performance in the presence of model uncertainties using three methods: RBFNN-based control, MNN-based control and model-based control, respectively

a Zoom-out
b Zoom-in

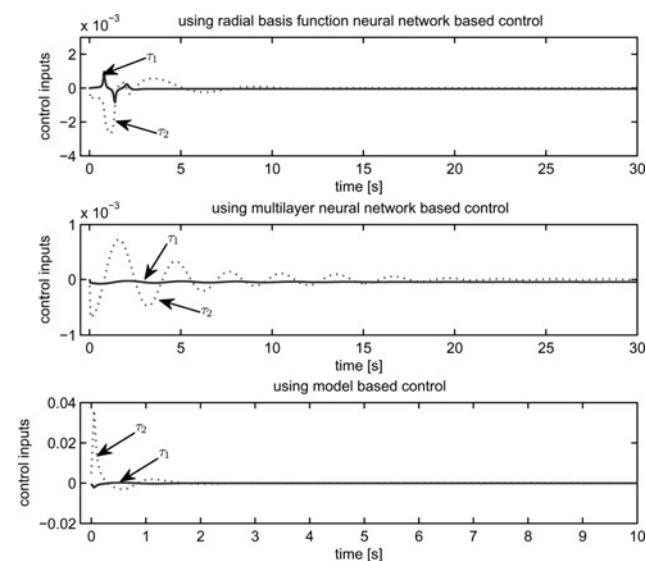


Figure 5 Control inputs for altitude and yaw angle tracking in the presence of model uncertainties using three methods: RBFNN-based control, MNN-based control and model-based control, respectively

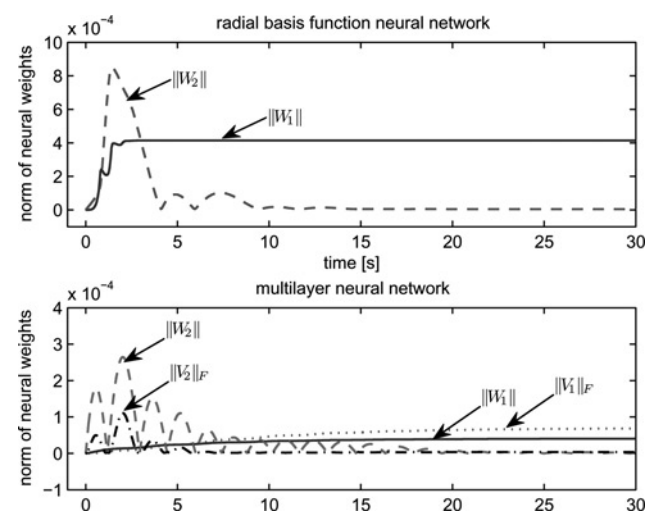


Figure 6 Norm of neural weights using RBFNN-based control and MNN-based control

trajectories in a short time about 20 s. This is because the model uncertainties can be learnt by RBFNN and MNN during the beginning 20 s. After that period, the uncertainties can be compensated for, and thus, the robustness to uncertainties is improved and the good tracking performance is achieved. In addition, Figs. 5 and 6 indicate the boundedness of the control actions and neural weights for all control methods.

5 Conclusion

In this paper, NN approximation-based control has been investigated for the helicopter altitude and yaw angle tracking in the presence of model uncertainties. Compared with the model-based control, which is sensitive to the accuracy of the model representation, NN approximation based control is tolerant of model uncertainties, and can be viewed as a key advantage over model-based control of helicopters, for which accurate modelling of helicopter dynamics is difficult, time-consuming and costly. Simulation results demonstrated that the helicopter is able to track altitude and yaw angle reference signals satisfactorily, with all other closed-loop signals bounded.

6 References

- [1] SIRA-RAMIREZ H., ZRIBI M., AHMAD S.: 'Dynamical sliding mode control approach for vertical flight regulation in helicopters', *IEE Proc. Control Theory Appl.*, 1994, **141**, pp. 19–24
- [2] DEVASIA S.: 'Output tracking with nonhyperbolic and near nonhyperbolic internal dynamics: helicopter hover control', *J. Guidance Control Dyn.*, 1997, **20**, (3), pp. 573–580
- [3] KOO T.J., SASTRY S.: 'Output tracking control design of a helicopter model based on approximate linearization'. Proc. IEEE Conf. Decision and Control, Tampa, Florida, 1998
- [4] CIVITA M.L., PAPAGEORGIOU G., MESSNER W., KANADE T.: 'Design and flight testing of a high-bandwidth H- ∞ loop shaping controller for a robotic helicopter'. Proc. AIAA Guidance, Navigation, and Control Conf. and Exhibit, August 2002
- [5] ISIDORI A., MARCONI L., SERRANI A.: 'Robust nonlinear motion control of a helicopter', *IEEE Trans. Autom. Control*, 2003, **48**, (3), pp. 413–426
- [6] VILCHIS J.A., BROGLIATO B., DZUL A., LOZANO R.: 'Nonlinear modelling and control of helicopters', *Automatica*, 2003, **39**, pp. 1583–1596
- [7] NARENDRA K.S., PARTHASARATHY K.: 'Identification and control of dynamic systems using neural networks', *IEEE Trans. Neural Netw.*, 1990, **1**, (1), pp. 4–27
- [8] LEVIN A.U., NARENDRA K.S.: 'Control of nonlinear dynamical systems using neural networks – part ii: observability, identification, and control', *IEEE Trans. Neural Netw.*, 1996, **7**, (1), pp. 30–42
- [9] LEWIS F.L., JAGANNATHAN S., YESILIDREK A.: 'Neural network control of robot manipulators and nonlinear systems' (Taylor and Francis, Philadelphia, PA, 1999)
- [10] GES.S., LEE T.H., HARRIS C.J.: 'Adaptive neural network control of robotic manipulators' (World Scientific, London, 1998)
- [11] GE S.S., HANG C.C., LEE T.H., ZHANG T.: 'Stable adaptive neural network control' (Kluwer Academic Publisher, Boston, 2002)
- [12] FARRELL J.A., POLYCARPOU M.M.: 'Adaptive approximation based control' (Wiley, Hoboken, NJ, 2006)
- [13] KIM B.S., CALISE A.J.: 'Nonlinear flight control using neural networks', *AIAA J. Guid. Control Dyn.*, 1997, **20**, pp. 26–33
- [14] RYSDYK R.T., CALISE A.J.: 'Nonlinear adaptive flight control using neural networks', *IEEE Control Syst. Mag.*, 1998, **18**, pp. 14–25
- [15] HOVAKIMYAN N., NARDI F., CALISE A.: 'Adaptive output feedback control of uncertain nonlinear systems using single-hidden-layer neural networks', *IEEE Trans. Neural Netw.*, 2002, **13**, (6), pp. 1420–1431
- [16] ENNS R., SI J.: 'Helicopter trimming and tracking control using direct neural dynamic programming', *IEEE Trans. Neural Netw.*, 2003, **14**, (4), pp. 929–939
- [17] KANNAN S., JOHNSON E.: 'Adaptive trajectory-based flight control for autonomous helicopters'. Proc. 21st Digital Avionics Systems Conf., October 2002, pp. 8.D.1.1–8.D.1.12
- [18] JOHNSON E.N., KANNAN S.K.: 'Adaptive trajectory control for autonomous helicopters', *AIAA J. Guid. Control. Dyn.*, 2005, **28**, pp. 524–538
- [19] RAIMUNDEZ J.C., CAMANO J.L., BALTAR J.A.: 'MIMO output feedback adaptive neural network control of an autonomous scale model helicopter mounted in a 2DOF platform', *Proc. World Autom. Cong.*, 2004, **15**, pp. 215–222
- [20] TEE K.P., GE S.S., TAY E.H.: 'Adaptive neural network control for helicopters in vertical flight', *IEEE Trans. Control Systems Technol.*, 2008, **16**, (4), pp. 753–762
- [21] FUNAHASHI K.I.: 'On the approximate realization of continuous mappings by neural networks', *Neural Netw.*, 1989, **2**, pp. 183–192
- [22] NARENDRA K.S., ANNASWAMY A.M.: 'A new adaptive law for robust adaptation without persistent

excitation', *IEEE Trans. Autom. Control*, 1987, **32**, pp. 134–145

[23] NARENDRA K.S., ANNASWAMY A.M.: 'Stable adaptive systems' (Prentice Hall, Englewood Cliffs, NJ, 1989)

[24] LEWIS F.L., YESILDIREK A., LIU K.: 'Multilayer neural network robot controller with guaranteed tracking performance', *IEEE Trans. Neural Netw.*, 1996, **7**, (2), pp. 388–399

[25] SLOTINE J.-J.E., LI W.: 'Applied nonlinear control' (Prentice-Hall, Englewood Cliffs, NJ, 1991)

[26] GE S.S., ZHANG J.: 'Neural-network control of nonaffine nonlinear system with zero dynamics by state and output feedback', *IEEE Trans. Neural Netw.*, 2003, **14**, (4), pp. 900–918

[27] KHALIL H.K.: 'Nonlinear systems' (Prentice Hall, NJ, 2002, 3rd edn.)